

Spontaneous CP Violation in Lepton-sector: a common origin for θ_{13} , Dirac CP phase and leptogenesis

Biswajit Karmakar^{a,1}, Arunansu Sil^{a,2}

^a *Indian Institute of Technology Guwahati, 781039 Assam, India*

Abstract

A possible interplay between the two terms of the general type-II seesaw formula is exercised which leads to the generation of nonzero θ_{13} . The specific flavor structure of the model, guided by the $A_4 \times Z_4 \times Z_3$ symmetry and accompanied with the Standard Model singlet flavons, yields the conventional seesaw contribution to produce the tribimaximal lepton mixing which is further corrected by the presence of the $SU(2)_L$ triplet contribution to accommodate θ_{13} . We consider the CP symmetry to be spontaneously broken by the complex vacuum expectation value (vev) of a singlet field S . While the magnitude of its complex vev is responsible for generating θ_{13} , its phase part induces the low energy CP violating phase (δ) and the CP violation required for leptogenesis. Hence the triplet contribution, although sub-dominant, plays crucial role in providing a common source for non-zero θ_{13} , δ and CP-violation required for leptogenesis. We find that the recent hint for δ close to $3\pi/2$ is somewhat favored in this set-up though it excludes the exact equality with $3\pi/2$. We also discuss the generation of lepton asymmetry in this scenario.

1 Introduction

The question whether there exists an underlying principle to understand the pattern of lepton mixing, which is quite different from the quark mixing, demands the study of neutrino mass matrix as well as the charged lepton one into a deeper level. The smallness of neutrino masses can be well understood by the seesaw mechanism in a natural way. Type-I seesaw mechanism [1–4] provides the simplest possibility by extending the Standard Model (SM) with three right-handed (RH) neutrinos. An introduction of discrete symmetries into it may reveal the flavor structure of the neutrino and charged lepton mass matrix. For example, a type-I seesaw in conjugation with A_4 explains the tribimaximal lepton mixing pattern (TBM) [5] in presence of SM singlet flavon (charged under A_4) fields which get vacuum expectation values

¹k.biswajit@iitg.ernet.in

²asil@iitg.ernet.in

(v_e) [6–8]. However the original approach fails to accommodate the recent observation of non-zero θ_{13} [9–12]. In [13], we have shown that an extension of the Altarelli-Feruglio (AF) model [8] by one additional flavon field can be employed to have a nonzero θ_{13} consistent with the present experimental results. The set-up also constraints the two Majorana phases involved in the lepton mixing matrix. The deviation of the TBM pattern is achieved through a deformation of the RH neutrino mass matrix compared to the original one. On the other hand, within the framework of a general type-II seesaw mechanism (where both RH neutrinos and $SU(2)_L$ triplet Higgs are present), light neutrino mass depends upon comparative magnitude of the pure type-I (mediated by heavy RH neutrinos) and triplet contributions. This interplay is well studied in the literature [14–23]. In recent years keeping in mind that θ_{13} is nonzero, efforts have been given to realize leptogenesis [24–30] and linking it with θ_{13} in models based on type-II seesaw [31].

In this article, we focus on the generation of light neutrino mass matrix through a type-II seesaw mechanism [32–35]. The fields content of the SM is extended with three right-handed neutrinos, one $SU(2)_L$ triplet and a set of SM singlet flavon fields. A flavor symmetry $A_4 \times Z_4 \times Z_3$ is considered. The type-II seesaw mechanism therefore consists of the conventional type-I seesaw contribution (m_ν^I) along with the triplet contribution (m_ν^{II}) to the neutrino mass matrix. Here we find the type-I contribution alone can generate the TBM mixing pattern, where the charged lepton mass matrix is a diagonal one. Then we have shown that the same flavor symmetry allows us to have a deviation from the conventional type-I contribution, triggered by the $SU(2)_L$ triplet’s vev. We have found that this deviation is sufficient enough to keep θ_{13} at an acceptable level [36–38]. We mostly consider the triplet contribution to the light neutrino mass is subdominant compared to the conventional type-I contribution.

We further assume that apart from the flavons (SM singlets charged under A_4) involved, there is a A_4 singlet (as well as SM gauge singlet) field S , which gets a complex vacuum expectation value and thereby responsible for spontaneous CP violation³ at high scale [47–52]. All other flavons have real vevs and all the couplings involved are considered to be real. It turns out that the magnitude of this complex vacuum expectation value of S is responsible for the deviation of TBM by generating nonzero value of θ_{13} in the right ballpark. On the other hand, the phase associated with it generates the Dirac CP violating phase in the lepton sector. So in a way, the triplet contribution provides a unified source for CP violation and nonzero θ_{13} . In lepton sector, the other possibilities where CP violation can take place, involves complex vev of Higgs triplets [53,54], or when a Higgs bi-doublet (particularly in left-right models) gets

³Earlier it has been shown that the idea of spontaneous CP violation [39] can be used to solve strong CP problem [40, 41]. Latter it has been successfully applied on models based on $SO(10)$ [42, 43] and other extensions of Standard Model [44–46].

complex vev [55] or in a mixed situation [56–58]. However, we will concentrate in a situation where a scalar singlet S present in the theory gets complex vev as in [48]. We have also studied the lepton asymmetry production through the decay of the heavy triplet involved. The decay of the triplet into two leptons contributes to the asymmetry where the virtual RH neutrinos are involved in the loop. This process is effective when the triplet is lighter than all the RH neutrinos. It turns out that sufficient lepton asymmetry can be generated in this way. On the other hand if the triplet mass is heavier than the RH neutrino masses, the lightest RH neutrino may be responsible for producing lepton asymmetry where the virtual triplet is contributing in the one loop diagram.

In [48], authors investigated a scenario where the triplet vevs are the sole contribution to the light neutrino mass and a single source of spontaneous CP violation was considered. There, it was shown that the low energy CP violating phase and the CP violation required for leptogenesis both are governed by the argument of the complex vev of that scalar field. The nonzero value of θ_{13} however followed from a perturbative deformation of the vev alignment of the flavons involved. Here in our scenario, the TBM pattern is realized by the conventional type-I contribution. Therefore in the TBM limit, θ_{13} is zero in our set-up. Also there is no CP violating phase in this limit as all the flavons involved in m_ν^I are carrying real vevs, and hence no lepton asymmetry as well. Now once the triplet contribution (m_ν^{II}) is switched on, not only the θ_{13} , but also the leptonic CP violation turn out to be nonzero. For generating lepton asymmetry, two triplets were essential in [48], while we could explain the lepton asymmetry by a single triplet along with the presence of RH neutrinos. In this case, the RH neutrinos are heavier compared to the mass of the triplet involved.

The paper is organized as follows. In section 2, we provide the status of the neutrino mixing and the mass squared differences. Then in section 3, we describe the set-up of the model followed by constraining the parameter space of the framework from neutrino masses and mixing in section 4. In section 5, we describe how one can obtain lepton asymmetry out of this construction. Finally we conclude in section 6.

2 Status of Neutrino Masses and Mixing:

Here we summarize the neutrino mixing parameters and their present status. The neutrino mass matrix m_ν , in general, can be diagonalized by the U_{PMNS} matrix (in the basis where charged lepton mass matrix is diagonal) as $m_\nu = U_{PMNS}^* \text{diag}(m_1, m_2, m_3) U_{PMNS}^\dagger$, where m_1, m_2, m_3 are the real mass eigenvalues for light neutrinos. The standard parametrization

of the U_{PMNS} matrix [59] is given by

$$U_{PMNS} = \begin{pmatrix} c_{12}c_{13} & s_{12}c_{13} & s_{13}e^{-i\delta} \\ -s_{12}c_{23} - c_{12}s_{13}s_{23}e^{i\delta} & c_{12}c_{23} - s_{12}s_{13}s_{23}e^{i\delta} & c_{13}s_{23} \\ s_{12}s_{23} - c_{12}s_{13}c_{23}e^{i\delta} & -c_{12}s_{23} - s_{12}s_{13}c_{23}e^{i\delta} & c_{13}c_{23} \end{pmatrix} \begin{pmatrix} 1 & 0 & 0 \\ 0 & e^{i\alpha_{21}/2} & 0 \\ 0 & 0 & e^{i\alpha_{31}/2} \end{pmatrix}, (2.1)$$

where $c_{ij} = \cos \theta_{ij}$, $s_{ij} = \sin \theta_{ij}$, the angles $\theta_{ij} = [0, \pi/2]$, $\delta = [0, 2\pi]$ is the CP-violating Dirac phase while α_{21} and α_{31} are the two CP-violating Majorana phases. The mixing angles θ_{12} ,

Oscillation parameters	best fit	1σ range	3σ range
Δm_{21}^2 [10^{-5} eV 2]	7.60	7.42–7.79	7.11–8.18
$ \Delta m_{31}^2 $ [10^{-3} eV 2]	2.48 (NH)	2.41 – 2.53	2.30 – 2.65
	2.38 (IH)	2.32 – 2.43	2.20 – 2.54
$\sin^2 \theta_{12}$	0.323	0.307–0.339	0.278–0.375
$\sin^2 \theta_{23}$	0.567 (NH)	0.439–0.599	0.392–0.643
	0.573 (IH)	0.530–0.598	0.403–0.640
$\sin^2 \theta_{13}$	0.0234 (NH)	0.0214–0.0254	0.0177–0.0294
	0.0240 (IH)	0.0221–0.0259	0.0183–0.0297

Table 1: Summary of neutrino oscillation parameters for normal and inverted neutrino mass hierarchies from the analysis of [38].

θ_{23} and the two mass-squared differences $\Delta m_{12}^2 (\equiv m_2^2 - m_1^2)$, $\Delta m_{31}^2 (\equiv m_3^2 - m_1^2)$ have been well measured at several neutrino oscillation experiments [60]. Recently the other mixing angle θ_{13} is also reported to be of sizable magnitude [9–12]. Very recently, we start to get hint for nonzero Dirac CP phase [12,36–38]. From the updated global analysis [38] involving all the data from neutrino experiments, the 1σ and 3σ ranges of mixing angles and the mass-squared differences are mentioned (NH and IH stand for the normal and inverted mass hierarchies respectively) in Table 1. The result by Planck [61] from the analysis of cosmic microwave background (CMB) also sets an upper limit on the sum of the three neutrino masses as given by, $\Sigma_i m_{\nu_i} < 0.23$ eV. The result from neutrinoless double beta decay by KamLAND-Zen [62] and EXO-200 [63] indicates a limit on the effective neutrino mass parameter $|m_{ee}|$ as, $|m_{ee}| < (0.14 - 0.28)$ eV at 90% CL and $|m_{ee}| < (0.19 - 0.45)$ eV at 90% CL respectively.

3 The Model

Our starting point is the conventional type-I seesaw mechanism to explain the smallness of light neutrino masses which further predicts a tribimaximal mixing (TBM) pattern in the lepton sector. For this part, we use the original AF model [8] by introducing a discrete A_4 symmetry and A_4 triplet flavon fields ϕ_S, ϕ_T along with a singlet ξ field. Of course three right

handed neutrinos (N_R) are also incorporated. In addition, we include a $SU(2)_L$ triplet field (Δ) with hypercharge unity, the vev of which produces an additional contribution (hereafter called the triplet contribution) to the light neutrino mass. So our set-up basically involves a general type-II seesaw,

$$m_\nu = m_\nu^{II} + m_\nu^I = m_\nu^{II} - m_D^T M_R^{-1} m_D, \quad (3.1)$$

where m_ν^I is the typical type-I term and m_ν^{II} is the triplet contribution. To realize both, the relevant Lagrangian for generation of m_ν can be written as,

$$-\mathcal{L} = Y_D \bar{L} \tilde{H} N_R + \frac{1}{2} M_R \bar{N}_R^c N_R + (Y_\Delta)_{ij} L_i^T C \Delta L_j, \quad (3.2)$$

so that $m_\nu^{II} = 2Y_\Delta u_\Delta$ and $m_D = Y_D v$, where u_Δ and v are the vevs of the triplet Δ and SM Higgs doublet (H) respectively. Y_D and Y_Δ correspond to the Yukawa matrices for the Dirac mass and triplet terms respectively, the flavor structure of which are solely determined by the discrete symmetries imposed on the fields involved in the model. M_R is the Majorana mass of the RH neutrinos. In the following subsection, we discuss in detail how the flavor structure of Y_D, Y_Δ and M_R are generated with the flavon fields. A discrete symmetry $Z_4 \times Z_3$ is also present in our model and two other SM singlet fields ξ' and S are introduced. These additional fields and the discrete symmetries considered play crucial role in realizing a typical structure of the triplet contribution to the light neutrino mass matrix as we will see below. Among all these scalar fields present, only the S field is assumed to have a complex vev while all other vevs are real. The framework is based on the SM gauge group extended with the $A_4 \times Z_4 \times Z_3$ symmetry. The field contents and charges under the symmetries imposed are provided in Table 2.

Field	e_R	μ_R	τ_R	L	N_R	H	Δ	ϕ_S	ϕ_T	ξ	ξ'	S
A_4	1	$1''$	$1'$	3	3	1	1	3	3	1	$1'$	1
Z_4	-1	-1	-1	i	i	1	$-i$	-1	$-i$	-1	i	-1
Z_3	ω	ω	ω	ω	ω	1	ω^2	ω	1	ω	ω^2	1

Table 2: Fields content and transformation properties under the symmetries imposed on the model.

With the above fields content, the charged lepton Lagrangian is described by,

$$\mathcal{L}_l = \frac{y_e}{\Lambda} (\bar{L} \phi_T) H e_R + \frac{y_\mu}{\Lambda} (\bar{L} \phi_T)' H \mu_R + \frac{y_\tau}{\Lambda} (\bar{L} \phi_T)'' H \tau_R, \quad (3.3)$$

to the leading order, where Λ is the cut-off scale of the theory and y_e, y_μ and y_τ are the respective coupling constants. Terms in the first parenthesis represent products of two A_4

triplets, which further contracts with A_4 singlets $1, 1''$ and $1'$ corresponding to e_R, μ_R and τ_R respectively to make a true singlet under A_4 . Once the flavons ϕ_S and ϕ_T get the vevs along a suitable direction as (u_S, u_S, u_S) and $(u_T, 0, 0)$ respectively⁴, it leads to a diagonal mass matrix for charged leptons, once the Higgs vev v is inserted. Below we will first summarize how the TBM mixing is achieved followed by the triplet contribution in the next subsection. The requirement of introducing SM singlet fields will be explained subsequently while discussing the flavor structure of neutrino mass matrix in detail.

3.1 Type-I Seesaw and Tribimaximal Mixing

The relevant Lagrangian for the type-I seesaw in the neutrino sector is given by,

$$\mathcal{L}_I = y\bar{L}\tilde{H}N_R + x_A\xi\bar{N}_R^cN_R + x_B\phi_S\bar{N}_R^cN_R, \quad (3.4)$$

where y, x_A and x_B are the coupling constants. After the ξ and ϕ_S fields get vevs and the electroweak vev v is included, it yields the following flavor structure for Dirac (m_D) and Majorana (M_R) mass matrices,

$$m_D = Y_D v = yv \begin{pmatrix} 1 & 0 & 0 \\ 0 & 0 & 1 \\ 0 & 1 & 0 \end{pmatrix} \quad \text{and} \quad M_R = \begin{pmatrix} a + 2b/3 & -b/3 & -b/3 \\ -b/3 & 2b/3 & a - b/3 \\ -b/3 & a - b/3 & 2b/3 \end{pmatrix}, \quad (3.5)$$

with $a = 2x_A\langle\xi\rangle = 2x_A u_\xi, b = 2x_B u_S$. The A_4 multiplication rules that results to this flavor structure can be found in [13]. Therefore the contribution toward light neutrino mass that results from the type-I seesaw mechanism is found to be,

$$\begin{aligned} m_\nu^I &= -m_D^T M_R^{-1} m_D \\ &= -y^2 v^2 \begin{pmatrix} \frac{3a+b}{3a(a+b)} & \frac{b}{3a(a+b)} & \frac{b}{3a(a+b)} \\ \frac{b}{3a(a+b)} & -\frac{b(2a+b)}{3a(a^2-b^2)} & \frac{3a^2+ab-b^2}{3a(a^2-b^2)} \\ \frac{b}{3a(a+b)} & \frac{3a^2+ab-b^2}{3a(a^2-b^2)} & -\frac{b(2a+b)}{3a(a^2-b^2)} \end{pmatrix}. \end{aligned} \quad (3.6)$$

Note that this form of m_ν^I indicates that the corresponding diagonalizing matrix would be nothing but the TBM mixing matrix of the form [5]

$$U_{TB} = \begin{pmatrix} \sqrt{\frac{2}{3}} & \frac{1}{\sqrt{3}} & 0 \\ -\frac{1}{\sqrt{6}} & \frac{1}{\sqrt{3}} & -\frac{1}{\sqrt{2}} \\ -\frac{1}{\sqrt{6}} & \frac{1}{\sqrt{3}} & \frac{1}{\sqrt{2}} \end{pmatrix}. \quad (3.7)$$

⁴The typical vev alignments of ϕ_S and ϕ_T are assumed here. We expect the minimization of the potential involving ϕ_S and ϕ_T can produce this by proper tuning of the parameters involved in the potential. However the very details of it are beyond the scope of this paper.

As a characteristic of typical A_4 generated structure, the RH neutrinos mass matrix is as well diagonalized by the U_{TB} . In order to achieve the real and positive mass eigenvalues, the corresponding rotation U_R is provided on M_R as $U_R^T M_R U_R = M_R^{\text{diag}} = \text{diag}(a+b, a, a-b)$ with $U_R = U_{TB} \text{diag}(1, 1, e^{-i\pi/2})$ once $a > b$ is considered. On the other hand for $a < b$; through $U_R = U_{TB}$ itself, the real and positive eigenvalues of M_R [$M_R^{\text{diag}} = \text{diag}(a+b, a, b-a)$] can be obtained. This would be useful when we will consider the decay of the RH neutrinos for leptogenesis in Section 5.

3.2 Triplet Contribution and Type-II seesaw

The leading order Lagrangian invariant under the symmetries imposed, that describes the triplet contribution to the light neutrino mass matrix (m_ν^{II}), is given by,

$$\mathcal{L}_{II} = \frac{1}{\Lambda^2} \Delta L^T \bar{L} (x_1 S + x'_1 S^*) \xi', \quad (3.8)$$

where x_1 and x'_1 are the couplings involved. Here ξ' develops a vev $u_{\xi'}$ and the singlet S is having a complex vev $\langle S \rangle = v_S e^{i\alpha_S}$. As we have mentioned before, the vev of S provides the unique source of CP violation as all other vevs and couplings are assumed to be real. CP is therefore assumed to be conserved in all the terms involved in the Lagrangian. Similar to [48], CP is spontaneously broken by the complex vev of the S field. After plugging all these vevs, the above Lagrangian in Eq.(3.8) contributes to the following Yukawa matrix for the triplet Δ as given by,

$$Y_\Delta = h \begin{pmatrix} 0 & 0 & 1 \\ 0 & 1 & 0 \\ 1 & 0 & 0 \end{pmatrix}, \quad h = \frac{1}{\Lambda^2} u_{\xi'} v_S (x_1 e^{i\alpha_S} + x'_1 e^{-i\alpha_S}). \quad (3.9)$$

This specific structure follows from the A_4 charge assignments of various fields present in Eq.(3.8) and is instrumental in providing nonzero θ_{13} as we will see shortly.

Before discussing the vev of the Δ field, let us describe the complete scalar potential V , including the triplet Δ obeying the symmetries imposed, is given by,

$$V = V_S + V_H + V_\Delta + V_{SH} + V_{S\Delta} + V_{\Delta H}, \quad (3.10)$$

where

$$\begin{aligned}
V_S &= \mu_S^2(S^2 + S^{*2}) + m_S^2 S^* S + \lambda_1(S^4 + S^{*4}) + \lambda_2 S^* S(S^2 + S^{*2}) + \lambda_3(S^* S)^2, \\
V_H &= m_H^2 H^\dagger H + \lambda_4(H^\dagger H)^2, \\
V_\Delta &= M_\Delta^2 \text{Tr}(\Delta^\dagger \Delta) + \lambda_5[\text{Tr}(\Delta^\dagger \Delta)]^2, \\
V_{SH} &= \lambda_6(S^* S)H^\dagger H + \lambda_7(S^2 + S^{*2})(H^\dagger H), \\
V_{S\Delta} &= \text{Tr}(\Delta^\dagger \Delta)[\lambda_8(S^2 + S^{*2}) + \lambda_9 S^* S], \\
V_{\Delta H} &= \lambda_{10}(H^\dagger H)\text{Tr}(\Delta^\dagger \Delta) + \lambda_{11}(H^\dagger \Delta^\dagger \Delta H) + \left(-\frac{\mu}{\Lambda} \tilde{H}^T \Delta \tilde{H} \phi_S \phi_T + h.c.\right). \quad (3.11)
\end{aligned}$$

The above potential contains several dimensionful (denoted by $\mu_S, m_{S,H}, M_\Delta$) and dimensionless parameters (as $\lambda_{i=1,2,\dots,11}$ and μ), which are all considered to be real. Similar to [48], here also it can be shown that the S field gets a complex vev for a choice of parameters involved in V_S as $m_S^2 < 0, \mu_S \simeq 0$ and $\lambda_3 > 2\lambda_1 > 0$. However contrary to [48], here we have only a single triplet field Δ . Once the ϕ_S, ϕ_T get vevs, the last term of $V_{\Delta H}$ results into an effective $\Delta H H$ interaction which would be important for leptogenesis. The vev of the triplet Δ is obtained by minimizing the relevant terms⁵ from V after plugging the vevs of the flavons and is given by

$$\langle \Delta^0 \rangle \equiv u_\Delta = \eta \frac{v^2}{M_\Delta^2} \quad \text{and} \quad \eta = \frac{\mu}{\Lambda} u_S u_T. \quad (3.12)$$

Using Eqs.(3.9) and (3.12), the triplet contribution to the light neutrino mass matrix follows from the Lagrangian $\mathcal{L}_{\mathcal{I}\mathcal{I}}$ as

$$m_\nu^{\mathcal{I}\mathcal{I}} = \begin{pmatrix} 0 & 0 & d \\ 0 & d & 0 \\ d & 0 & 0 \end{pmatrix}, \quad (3.13)$$

where

$$d = 2hu_\Delta = 2h\eta \frac{v^2}{M_\Delta^2}. \quad (3.14)$$

Note that only the triplet contribution (d) involves the phase due to the involvement of $\langle S \rangle$ in h , while the entire type-I contribution $m_\nu^{\mathcal{I}}$ remains real. Therefore the term d serves as the unique source of generating all the CP-violating phases involved in neutrino as well as in lepton mixing. This will be clear once we discuss the neutrino mixing in the subsequent section. Now we can write down the entire contribution to the light neutrino mass as,

$$m_\nu = -y^2 v^2 \begin{pmatrix} \frac{3a+b}{3a(a+b)} & \frac{b}{3a(a+b)} & \frac{b}{3a(a+b)} \\ \frac{b}{3a(a+b)} & -\frac{b(2a+b)}{3a(a^2-b^2)} & \frac{3a^2+ab-b^2}{3a(a^2-b^2)} \\ \frac{b}{3a(a+b)} & \frac{3a^2+ab-b^2}{3a(a^2-b^2)} & -\frac{b(2a+b)}{3a(a^2-b^2)} \end{pmatrix} + \begin{pmatrix} 0 & 0 & d \\ 0 & d & 0 \\ d & 0 & 0 \end{pmatrix}. \quad (3.15)$$

⁵We consider couplings $\lambda_{8,9} \ll 1$.

4 Constraining parameters from neutrino mixing

In this section, we discuss how the neutrino masses and mixing can be obtained from the m_ν mentioned above. Keeping in mind that m_ν^I can be diagonalized by U_{TB} , we first perform a rotation by U_{TB} on the explicit form of the light neutrino mass matrix obtained in Eq.(3.15) and the rotated m_ν is found to be

$$m'_\nu = U_{TB}^T m_\nu U_{TB} = \begin{pmatrix} -\frac{ad+bd+2v^2y^2}{2(a+b)} & 0 & \frac{\sqrt{3}d}{2} \\ 0 & d - \frac{v^2y^2}{a} & 0 \\ \frac{\sqrt{3}d}{2} & 0 & \frac{ad-bd+2v^2y^2}{2(a-b)} \end{pmatrix}, \quad (4.1)$$

$$= \begin{pmatrix} -\frac{d}{2} - \frac{k}{(1+\alpha)} & 0 & \frac{\sqrt{3}d}{2} \\ 0 & d - k & 0 \\ \frac{\sqrt{3}d}{2} & 0 & \frac{d}{2} + \frac{k}{(1-\alpha)} \end{pmatrix}. \quad (4.2)$$

Here, we define the parameters $\alpha = b/a$ and $k = v^2y^2/a$ which are real and positive as part of the type-I contribution. We note that a further rotation by U_1 (another unitary matrix) in the 13 plane is required to diagonalize the light neutrino mass matrix, $U_1^T m'_\nu U_1 = m_\nu^{\text{diag}}$. With a form of U_1 as

$$U_1 = \begin{pmatrix} \cos \theta & 0 & \sin \theta e^{-i\psi} \\ 0 & 1 & 0 \\ -\sin \theta e^{i\psi} & 0 & \cos \theta \end{pmatrix}, \quad (4.3)$$

we have, $(U_{TB}U_1)^T m_\nu U_{TB}U_1 = \text{diag}(m_1 e^{i\gamma_1}, m_2 e^{i\gamma_2}, m_3 e^{i\gamma_3})$, where $m_{i=1,2,3}$ are the real and positive eigenvalues and $\gamma_{i=1,2,3}$ are the phases associated to these mass eigenvalues. We can therefore extract the neutrino mixing matrix U_ν as,

$$U_\nu = U_{TB}U_1U_m = \begin{pmatrix} \sqrt{\frac{2}{3}} \cos \theta & \frac{1}{\sqrt{3}} & \sqrt{\frac{2}{3}} e^{-i\psi} \sin \theta \\ -\frac{\cos \theta}{\sqrt{6}} + \frac{e^{i\psi} \sin \theta}{\sqrt{2}} & \frac{1}{\sqrt{3}} & -\frac{\cos \theta}{\sqrt{2}} - \frac{e^{-i\psi} \sin \theta}{\sqrt{6}} \\ -\frac{\cos \theta}{\sqrt{6}} - \frac{e^{i\psi} \sin \theta}{\sqrt{2}} & \frac{1}{\sqrt{3}} & \frac{\cos \theta}{\sqrt{2}} - \frac{e^{-i\psi} \sin \theta}{\sqrt{6}} \end{pmatrix} U_m \quad (4.4)$$

where $U_m = \text{diag}(1, e^{i\alpha_{21}/2}, e^{i\alpha_{31}/2})$ is the Majorana phase matrix with $\alpha_{21} = (\gamma_1 - \gamma_2)$ and $\alpha_{31} = (\gamma_1 - \gamma_3)$, one common phase being irrelevant. As the charged lepton mass matrix is a diagonal one, we can now compare this U_ν with the standard parametrization of lepton mixing matrix U_{PMNS} . The U_{PMNS} is therefore given by $U_{PMNS} = U_P U_\nu$, where we need to multiply the U_ν matrix by a diagonal phase matrix U_P [64] from left so that the U_{PMNS} excluding the Majorana phase matrix, can take the standard form where 22 and 33 elements are real as in Eq.(2.1). Hence we obtain the usual (in A_4 models) correlation [65] between

the angles and CP violating Dirac phase δ as given by

$$\sin \theta_{13} = \sqrt{\frac{2}{3}} |\sin \theta|, \quad \sin^2 \theta_{12} = \frac{1}{3(1 - \sin^2 \theta_{13})}, \quad (4.5)$$

$$\sin^2 \theta_{23} = \frac{1}{2} + \frac{1}{\sqrt{2}} \sin \theta_{13} \cos \delta, \quad \delta = \arg[(U_1)_{13}]. \quad (4.6)$$

The angle θ and phase ψ associated with U_1 can now be linked with the parameters involved in m_ν . For this we first rewrite the triplet contribution d as $d = |d|e^{i\phi_d}$ and define a parameter $\beta = |d|/k$ (hence β is real). This parameter indicates the relative size of the triplet contribution to the type-I contribution when $\alpha \leq 1$. As U_1 diagonalizes the m'_ν matrix, after some involved algebra, we finally get,

$$\tan 2\theta = \frac{\sqrt{3} [1 - (1 - \alpha^2) \cos^2 \phi_d]^{1/2}}{\alpha \frac{2}{\beta(1 - \alpha^2)} + \cos \phi_d} \quad \text{and} \quad \tan \psi = (\tan \phi_d)/\alpha. \quad (4.7)$$

$\sin \theta$ may take positive or negative value depending on the choices of α, β as evident from the first relation in Eq.(4.7). For $\sin \theta > 0$, we find $\delta = \psi$ using $\delta = \arg[(U_1)_{13}$ and the second relation of Eq.(4.7). On the other hand for $\sin \theta < 0$; δ and ψ are related by $\delta = \psi \pm \pi$. Therefore in both these cases we obtain $\tan \psi = \tan \delta$ and hence

$$\tan \delta = (\tan \phi_d)/\alpha. \quad (4.8)$$

In our set-up, the source of this CP-violating Dirac phase δ is through the phase α_S associated with $\langle S \rangle$. Note that $\tan \delta$ is related with $\tan \phi_d$ and α as seen from Eq.(4.8). Now from the relation $d = |d|e^{i\phi_d}$ and using Eq.(3.9) and (3.14), we obtain ϕ_d satisfying

$$\tan \phi_d = \frac{(x_1 - x'_1)}{(x_1 + x'_1)} \tan \alpha_S, \quad (4.9)$$

where x_1 and x'_1 are the coupling involved in Eq.(3.8).

As seen from Eqs.(4.5) and (4.7), we conclude that the U_{PMNS} parameters θ_{13} and δ depend on the model parameters α, β and ϕ_d . Note that we expect terms a and b ($\alpha = b/a$) to be of similar order of magnitude as both originated from the tree level Lagrangian (see Eqs.(3.4) and (3.5)). We categorize $\alpha < 1$ as case A, while $\alpha > 1$ is with case B. The other parameter β basically represents the relative order of magnitude between the triplet contribution ($|d|$) and the type-I contribution ($v^2 y^2/a$). Our framework produces the TBM mixing pattern to be generated solely by type-I seesaw and triplet contribution is present mainly to correct for the angle θ_{13} which is small compared to the other mixing angles. Therefore we consider that the triplet contribution is preferably the sub-dominant or at most comparable one. Therefore we expect the parameter β to be less than one. Although we discuss what happens when $\beta > 1$ in some cases, we will restrict ourselves with $\beta < 1$ for the

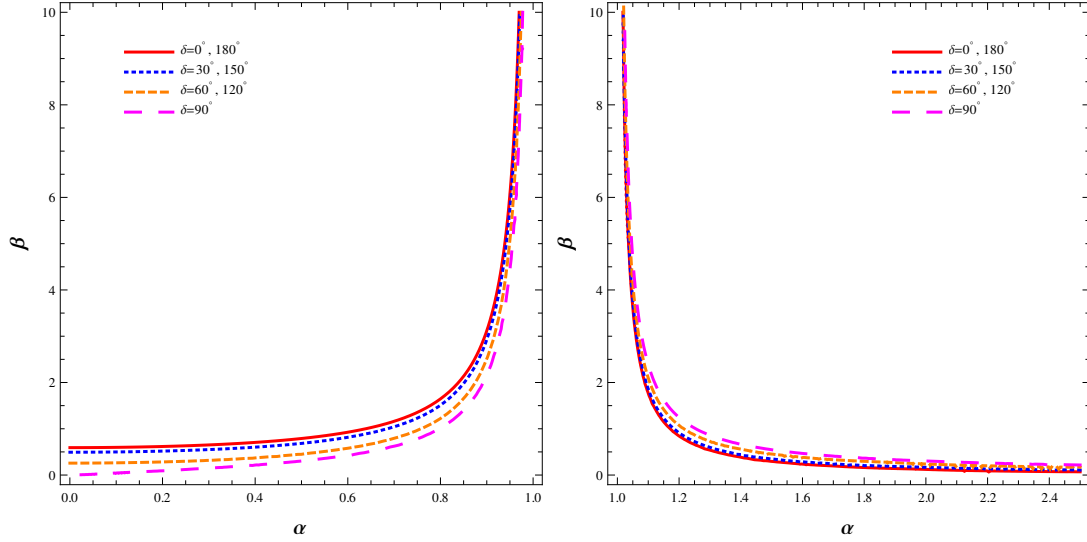


Figure 1: Contour plots for $\sin^2 \theta_{13} = 0.0234$ in the $\alpha - \beta$ plane for various choices of δ as indicated inside the figure. Left panel is for (A) $\alpha < 1$ and right panel is with (B) $\alpha > 1$.

most of the analyses involved later in this work. In Fig.1 left panel, we study the variation of α and β in order to achieve the best fit value of $\sin^2 \theta_{13} = 0.0234$ [38] while different values of δ are considered. In producing these plots, we have replaced the ϕ_d dependence in terms of α and δ by employing the second equation in Eq.(4.7) as $\psi = \delta$. Similarly in the right panel of Fig.1, contour plots for $\sin^2 \theta_{13} = 0.0234$ are depicted for $\alpha > 1$ with different values of δ . We find a typical contour plot for $\sin^2 \theta_{13}$ with a specific δ value coincides with the one with other δ values obtained from $|\pi - \delta|$. For example, one particular contour plot for $\delta = 30^\circ$ is repeated for $\delta = 150^\circ, 210^\circ, 330^\circ$.

Diagonalizing m'_ν in Eq.(4.2), the light neutrino masses turn out to be,

$$m_1 = k \left[\left(\frac{\alpha}{\pm(1-\alpha^2)} - \frac{p}{k} \right)^2 + \left(\frac{q}{k} \right)^2 \right]^{1/2}, \quad (4.10)$$

$$m_2 = k [1 + \beta^2 - 2\beta \cos \phi_d]^{1/2}, \quad (4.11)$$

$$m_3 = k \left[\left(\frac{\alpha}{\pm(1-\alpha^2)} + \frac{p}{k} \right)^2 + \left(\frac{q}{k} \right)^2 \right]^{1/2}, \quad (4.12)$$

where p and q are defined as,

$$\left(\frac{p}{k} \right)^2 = \frac{1}{2} \left(\frac{A}{k^2} + \sqrt{\frac{A^2}{k^4} + \frac{B^2}{k^4}} \right), \quad \left(\frac{q}{k} \right)^2 = \frac{1}{2} \left(-\frac{A}{k^2} + \sqrt{\frac{A^2}{k^4} + \frac{B^2}{k^4}} \right); \quad (4.13)$$

$$\frac{A}{k^2} = \beta^2 \cos 2\phi_d + \beta \frac{\cos \phi_d}{1-\alpha^2} + \frac{1}{(1-\alpha^2)^2}, \quad \frac{B}{k^2} = \beta^2 \sin 2\phi_d + \beta \frac{\sin \phi_d}{1-\alpha^2}. \quad (4.14)$$

The '+' sign in the expression of m_1 and m_3 is for $\alpha < 1$ (case A) where the '-' sign is

associated with $\alpha > 1$ (case B). The Majorana phases in U_m (see Eq.(4.4)) are found to be

$$\alpha_{21} = \tan^{-1} \left[\frac{q/k}{p/k \pm \frac{\alpha}{(\alpha^2-1)}} \right] - \tan^{-1} \left[\frac{\beta \sin \phi_d}{\beta \cos \phi_d - 1} \right], \quad (4.15)$$

$$\alpha_{31} = \pi + \tan^{-1} \left[\frac{q/k}{p/k \pm \frac{\alpha}{(\alpha^2-1)}} \right] - \tan^{-1} \left[\frac{q/k}{p/k \pm \frac{\alpha}{(1-\alpha^2)}} \right]. \quad (4.16)$$

Note that the redefined parameters p/k and q/k are functions of α , β and ϕ_d , while the mass eigenvalues m_i , depend on k as well.

The parameters α , β and ϕ_d can now be constrained by the neutrino oscillation data. To have a more concrete discussion, we consider the ratio, r , defined by $r = \frac{\Delta m_{\odot}^2}{|\Delta m_{atm}^2|}$, with $\Delta m_{\odot}^2 \equiv \Delta m_{21}^2 = m_2^2 - m_1^2$ and $|\Delta m_{atm}^2| \equiv \Delta m_{31}^2 = m_3^2 - m_1^2$ considering normal hierarchy. Following [38], the best fit values of $\Delta m_{\odot}^2 = 7.6 \times 10^{-5} \text{ eV}^2$ and $|\Delta m_{atm}^2| = 2.48 \times 10^{-3} \text{ eV}^2$ are used for our analysis. Using Eqs.(4.10-4.12), we have an expression for r as,

$$r = \frac{\pm(1-\alpha^2)k}{4\alpha p} \left[1 + \beta^2 - 2\beta \cos \phi_d - \left(\frac{\alpha}{\pm(1-\alpha^2)} - \frac{p}{k} \right)^2 - \left(\frac{q}{k} \right)^2 \right]. \quad (4.17)$$

Here also, ‘+’ corresponds to case A (*i.e.* with $\alpha < 1$) and ‘-’ is for case B (*i.e.*, when $\alpha > 1$). Interestingly we note that r depends on α , β and ϕ_d . Therefore using this expression of r , we can now have a contour plot for $r = 0.03$ [59] in terms of α and β for specific choices of δ as we can replace the ϕ_d dependence in terms of α and δ through Eq.(4.8). For $\alpha < 1$, this is shown in Fig.2, left panel and a similar plot is made for $\alpha > 1$ in the right panel. Although we argue that it is more natural to consider β to be less than one, in this plot we allow larger values of β as a completeness. With this, for $\alpha < 1$ (case A) we see the appearance of two separate contours of $r = 0.03$ with $\delta = 30^\circ$, one is for $\beta < 1$ and the other corresponds to $\beta > 1$. Similar plots are obtained for $\delta = 70^\circ$ as well. However these isolated contours become a connected one once the value of δ increases, e.g. at $\delta = 80^\circ$, it is shown in Fig.2, left panel. A similar pattern follows in case of $\alpha > 1$ case. Below we discuss the predictions of our model for case A (with $\alpha < 1$) and case B ($\alpha > 1$) separately.

4.1 Results for Case A

Note that we need to satisfy both the $\sin^2 \theta_{13}$ as well as the value of r obtained from the neutrino oscillation experiments. For this reason, if we consider the two contour plots (one for $r = 0.03$ and the other for $\sin^2 \theta_{13} = 0.0234$) together, then their intersection (denoted by (α, β)) should indicate a simultaneous satisfaction of these experimental data for a specific choice of δ . This is exercised in Fig.3. In the left panel of Fig.3, contour plots of r and $\sin^2 \theta_{13}$ are drawn in terms of α and β for two choices of $\delta = 20^\circ$ and 40° . We find that there is no such solution for (α, β) which satisfy both r and $\sin^2 \theta_{13}$ with $\alpha, \beta \lesssim 1$ in these cases. However

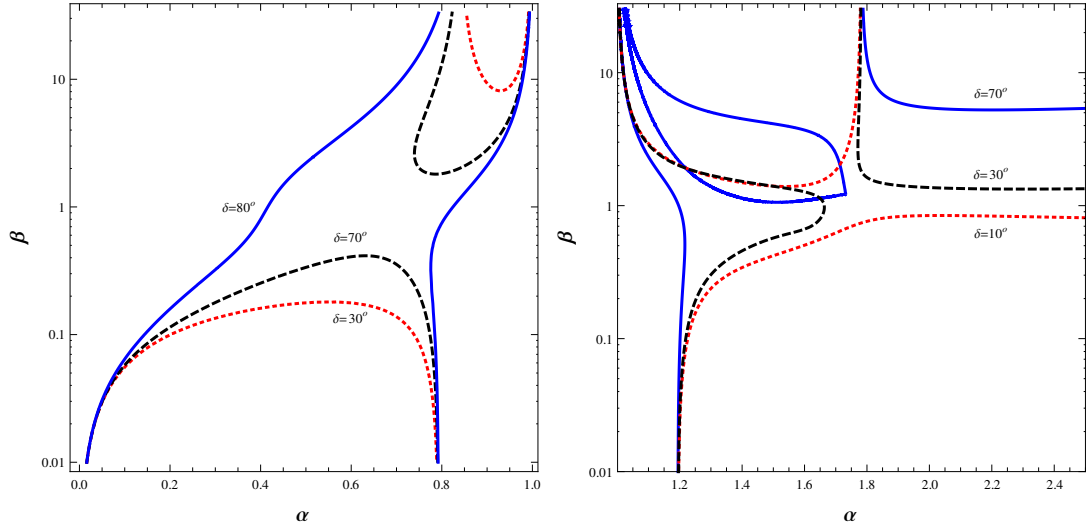


Figure 2: Contour plots for $r = 0.03$ are shown in the $\alpha - \beta$ plane. Here in the left panel (with $\alpha < 1$, case A) red (dotted), black (dashed) and blue (continuous) lines represent $\delta = 30^\circ, 70^\circ$ and 80° respectively. Similar contours are present for $|\pi - \delta|$ values of the CP violating Dirac phase. In the right panel (with $\alpha > 1$, case B) red (dotted), black (dashed) and blue (continuous) lines represent $\delta = 10^\circ, 30^\circ$ and 70° respectively.

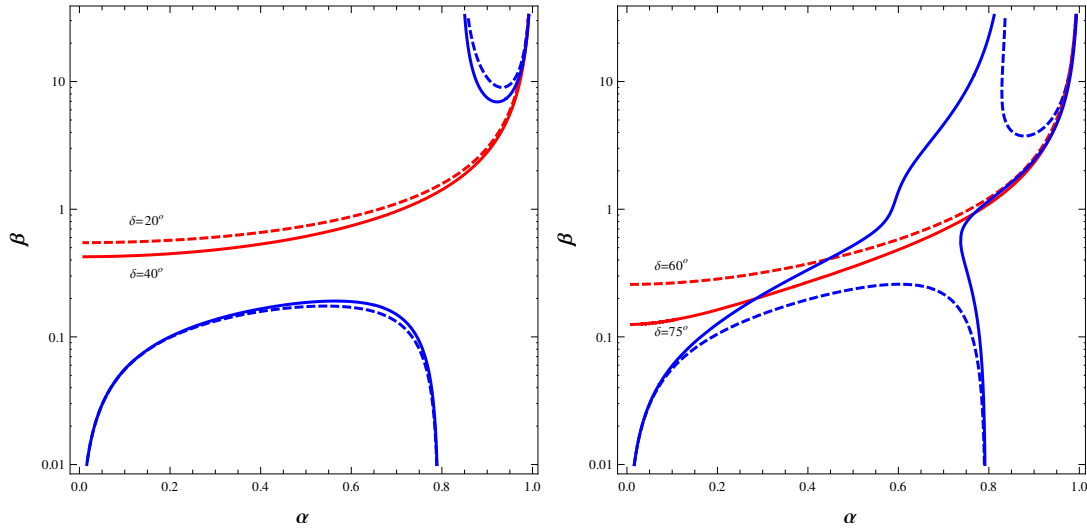


Figure 3: Contour plots for both $\sin^2 \theta_{13} = 0.0234$ and $r = 0.03$ in the $\alpha - \beta$ plane for various choices of δ . In the left panel, dotted and continuous lines represent $\delta = 20^\circ$ and 40° respectively. In the right panel, dashed and continuous lines represent contour plots for $\delta = 60^\circ$ and 75° respectively.

there exists solution for α very close to one with a pretty large value of β as mentioned in Table 3. This solution as we expect is not a natural one, not only for a large value of β , but also for its very fine tuned situation. Note that α requires to be sufficiently close (and

hence finely tuned) to one in this case. This situation can be understood from the fact that β being quite large ($\gg 1$), value of α has to be adjusted enough (see the involvement of the expression $\alpha/(1 - \alpha^2)$ in Eq.(4.17)) so as to compete with the β dependent terms to get $r \sim 0.03$. Similarly variation of $\sin^2 \theta_{13}$ is very sharp with respect to α (when close to 1) for large β . For example, a small change in α values ($\sim 1\%$) would induce a change in $\sin^2 \theta_{13}$ by an amount of 15% near the intersection region.

However the situation changes dramatically as we proceed for higher values of δ as can be seen from Fig.3, right panel. This figure is for two choices of $\delta = 60^\circ$ and 75° . We observe that with the increase of δ , the upper contour for r is extended toward downward direction and the lower one is pushed up, thereby providing a greater chance to have an intersection with the $\sin^2 \theta_{13}$ contour. We also note that the portion of $\sin^2 \theta_{13}$ contour for $\alpha < 1$ prefers a region with relatively small value of $\beta (< 1)$ as well. However a typical solution with both α and $\beta < 1$ appears when δ is closer to 75° . With this δ , we could see the lower and upper contours open up to form a connected one and we can have a solution for $(\alpha, \beta) \equiv (0.29, 0.2)$. In this case, there is one more intersection between the r and $\sin^2 \theta_{13}$ contours with $\alpha, \beta < 1$ as given by $(0.77, 0.93)$. When δ approaches 80° and up (till $\pi/2$) we have solutions with $\alpha, \beta < 1$.

δ	α	β	$\sum m_i(\text{eV})$
$20^\circ(160^\circ, 200^\circ, 340^\circ)$	0.99	28.26	0.0714
$40^\circ(140^\circ, 220^\circ, 320^\circ)$	0.99	20.94	0.0709
$60^\circ(120^\circ, 240^\circ, 300^\circ)$	0.98	11.16	0.0701
$75^\circ(105^\circ, 255^\circ, 285^\circ)$	0.94	3.70	0.0691
	0.77	0.93	0.0734
	0.29	0.20	0.1333
$80^\circ(100^\circ, 260^\circ, 280^\circ)$	0.16	0.11	0.1835
$82^\circ(98^\circ, 262^\circ, 278^\circ)$	0.12	0.09	0.2137
$85^\circ(95^\circ, 265^\circ, 275^\circ)$	0.07	0.05	0.2827

Table 3: α, β values at the intersection points of the r and $\sin^2 \theta_{13}$ contour plots are provided corresponding to different δ values. The sum of the light neutrino masses are also indicated in each case.

We have scanned the entire range of δ , from 0 to 2π and listed our findings in Table 3. For the δ values, we denote inside the first bracket those values of δ , for which the same set of solution points (α, β) are obtained. This is due to the fact that corresponding to a r or $\sin^2 \theta_{13}$ contour plot for a typical δ between 0 and 2π , the same plot is also obtained for other $|\pi - \delta|$ values. Accepting the solutions for which $\alpha, \beta < 1$ (i.e. those are not fine tuned with

large β), we find that the our setup then predicts an acceptable range of CP violating Dirac phase δ to be between $72^\circ - 82^\circ$, while the first quadrant is considered. For the whole range of δ between 0 and 2π , the allowed range therefore covers $72^\circ - 82^\circ$, $98^\circ - 108^\circ$, $252^\circ - 262^\circ$, $278^\circ - 288^\circ$. Note that δ between 83° and 90° (similarly regions of δ in other quadrants also) is ruled out from the constraints on the sum of the light neutrino mass mentioned in Table3. We will discuss about it shortly. Also the values of δ s like 0, π , 2π are disallowed in our setup as they would not produce any CP violation which is the starting point of our scenario. Again $\delta = \pi/2, 3\pi/2$ are not favored as we have not obtained any solution of α, β that satisfied both r and $\sin^2 \theta_{13}$. The same is true for the case with $\alpha > 1$.

We will now proceed to discuss the prediction of the model for the light neutrino masses and other relevant quantities in terms of the parameters involved in the set-up. For this, from now onward, we stick to the choice of $\delta = 80^\circ (\equiv 100^\circ, 260^\circ, 280^\circ)$ as a reference value for the Dirac CP violating phase. The r and $\sin^2 \theta_{13}$ contours for this particular δ is shown separately

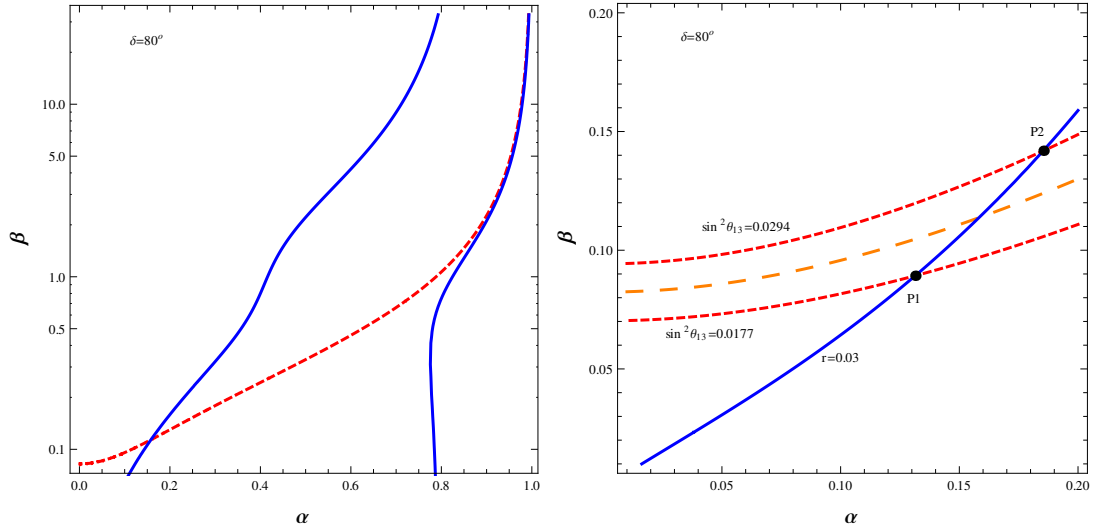


Figure 4: Left panel contains contour plots for best-fit values of r and $\sin^2 \theta_{13}$ for $\delta = 80^\circ$ in α - β plane. Here red dashed and blue continuous lines represent contours for $\sin^2 \theta_{13}$ and r respectively. The right panel is for best fit value of r (blue continuous line) and 3σ range of $\sin^2 \theta_{13}$ (denoted by two red dotted lines).

in Fig.(4), left panel. In Fig.(4) right panel we put the $\sin^2 \theta_{13}$ contours corresponding to the upper and lower values (denoted by red dotted lines) those are allowed by the 3σ range of $\sin^2 \theta_{13}$. Only a section of r contour is also incorporated which encompasses the (α, β) solution points. This plot provides a range for (α, β) once the 3σ patch of $\sin^2 \theta_{13}$ are considered. It starts from a set of values $(\sim 0.13, 0.09)$ (can be called a reference point P1) upto $(\sim 0.18, 0.14)$ (another reference point P2). Note that there is always a one-to-one

correspondence between the values of α and β , which falls on the line of r contour.

We have already noted that in the expression for r , parameters α, β and ϕ_d are present. Once we choose a specific δ , automatically it boils down to find α and β from Eq.(4.17). Although r is the ratio between Δm_{\odot}^2 and $|\Delta m_{atm}^2|$, we must also satisfy the mass-squared differences Δm_{\odot}^2 as well as $|\Delta m_{atm}^2|$ independently. For that we need to determine the value of the k parameter itself apart from its involvement in the ratio $\beta = |d|/k$ as evident from Eq.(4.10)-(4.12). For this purpose, with $\delta = 80^\circ$ while moving from P1 to P2 along the r contour in the right panel of Fig. 4, we find the values of α and correspondingly β which produce $r = 0.03$. Now using these values of (α, β) , we can evaluate the values of k for each such set which satisfies $\Delta m_{\odot}^2 = 7.6 \times 10^{-5} \text{eV}^2$. To obtain these values of k corresponding to (α, β) set, we employ Eqs.(4.10-4.11). The result is reflected in left panel of Fig.5, where

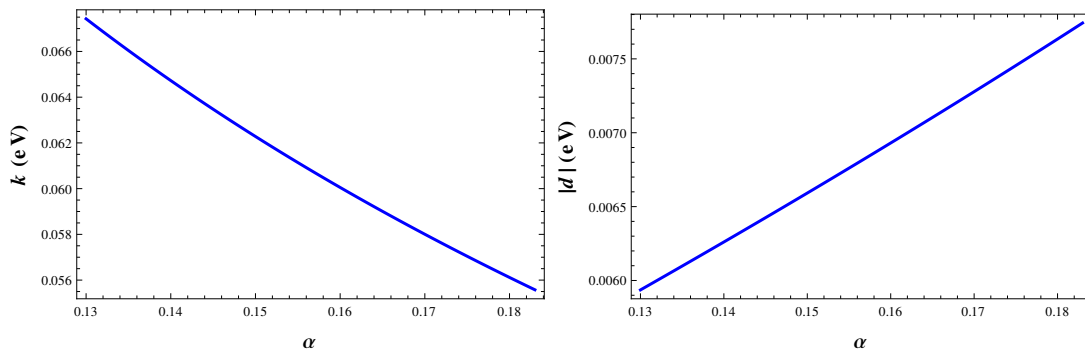


Figure 5: k vs. α (left-panel) and $|d|$ vs. α (right-panel) for $\delta = 80^\circ (\equiv 100^\circ, 260^\circ, 280^\circ)$.

we plot the required value of k in terms of its variation with α . In producing the plot, only a narrow range of α is considered which corresponds to the 3σ variation of $\sin^2 \theta_{13}$ as obtained from Fig.(4), right panel (*i.e.* from P1 to P2). Although we plot it against α , each value of α is therefore accompanied by a unique value of β , as we just explain. Once the variation of k in terms of α is known, we plot the variation of $|d|$ ($\beta = \beta k$) with α in Fig.5, right panel. Having the correlation between α and other parameters like β, k for a specific choice of δ is known, we are able to plot the individual light neutrino masses using Eqs.(4.10-4.12). This is done in Fig.6. The light neutrino masses satisfies normal mass hierarchy. We also incorporate the sum of light neutrino masses (Σm_i) to check its consistency with the cosmological limit set by Planck, $\Sigma m_i < 0.23 \text{ eV}$ [61]. In this particular case with $\delta = 80^\circ$ (also for $\delta = 100^\circ, 260^\circ, 280^\circ$), this limit is satisfied for the allowed range of α , it turns out that $\delta = 83^\circ$ and 97° (and similarly for $263^\circ - 277^\circ$) do not satisfy it as indicated in Table.3.

Now by using Eqs.(4.16-4.16), we estimate the Majorana phases⁶ α_{21} and α_{31} for $\delta = 80^\circ$,

⁶The source of these phases are the phase ϕ_d only.

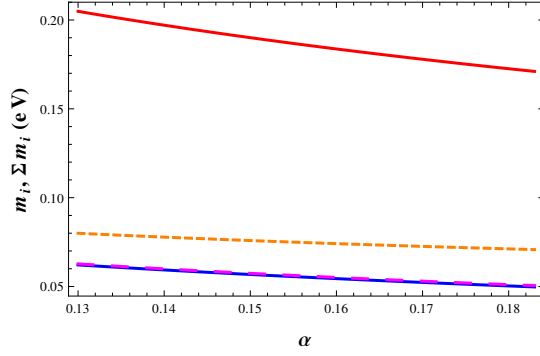


Figure 6: Light neutrino masses: m_1 (blue continuous line), m_2 (magenta large dashed), m_3 (orange dashed) and Σm_i (red continuous line) vs α for $\delta = 80^\circ (\equiv 100^\circ, 260^\circ, 280^\circ)$.

which appears in the effective neutrino mass parameter $|m_{ee}|$. $|m_{ee}|$ appears in evaluating the neutrinos double beta decay and is given by [59],

$$|m_{ee}| = \left| m_1^2 c_{12}^2 c_{13}^2 + m_2^2 s_{12}^2 c_{13}^2 e^{i\alpha_{21}} + m_3^2 s_{13}^2 e^{i(\alpha_{31}-2\delta)} \right|. \quad (4.18)$$

In Fig.7, we plot the prediction of $|m_{ee}|$ against α within its narrow range satisfying 3σ range of $\sin^2 \theta_{13}$ with $\delta = 80^\circ$. Here we obtain $0.050 \leq |m_{ee}| \leq 0.062$. This could be probed in future generation experiments providing a testable platform of the model itself.

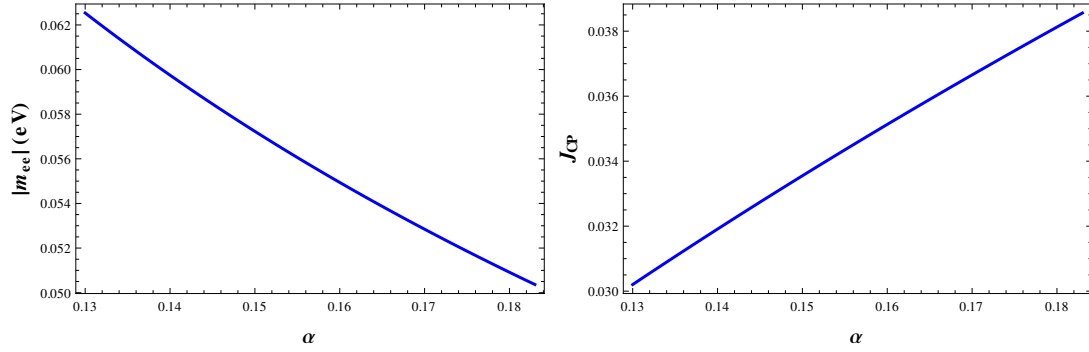


Figure 7: Effective neutrino mass parameter (left panel) and Jarlskog invariant (right panel) α for $\delta = 80^\circ (100^\circ, 260^\circ, 280^\circ)$.

It is known that presence of nonzero Dirac CP phase can trigger CP violation in neutrino oscillation at low energy. In standard parametrization, the magnitude of this CP violation can be estimated [59] through

$$\begin{aligned} J_{CP} &= \text{Im}[U_{\mu 3} U_{e 3}^* U_{e 2} U_{\mu 2}^*] \\ &= \frac{1}{8} \cos \theta_{13} \sin 2\theta_{12} \sin 2\theta_{23} \sin 2\theta_{13} \sin \delta. \end{aligned} \quad (4.19)$$

As in our model, the unique source of δ is the CP violating phase α_S in S , it is interesting to see the prediction of our model towards J_{CP} . Using the expression of J_{CP} in Eq. (4.19) along with Eqs.(4.5) and (4.6) we estimate J_{CP} in our model as shown in Fig.7, right panel with $\delta = 80^\circ$. Here also we include only that range of α which provides solutions corresponding to 3σ allowed range of $\sin^2 \theta_{13}$. However we scanned the entire range of α where the solutions exists for all allowed values of δ and find that J_{CP} in our model is predicted to be $0.03 < |J_{CP}| < 0.04$. This can be measured in future neutrino experiments.

4.2 Results for Case B

Similar to case A, we consider here the expression of r for $\alpha > 1$ from Eq.(4.17) to draw the contour plot for $r = 0.03$ in the $\alpha - \beta$ plane as shown in Fig.(8) while δ is fixed at different values. In the same plot we include the $\sin^2 \theta_{13} = 0.0234$ contour as well to find the set of parameters (α, β) corresponding to a fixed δ which satisfies the best fit values

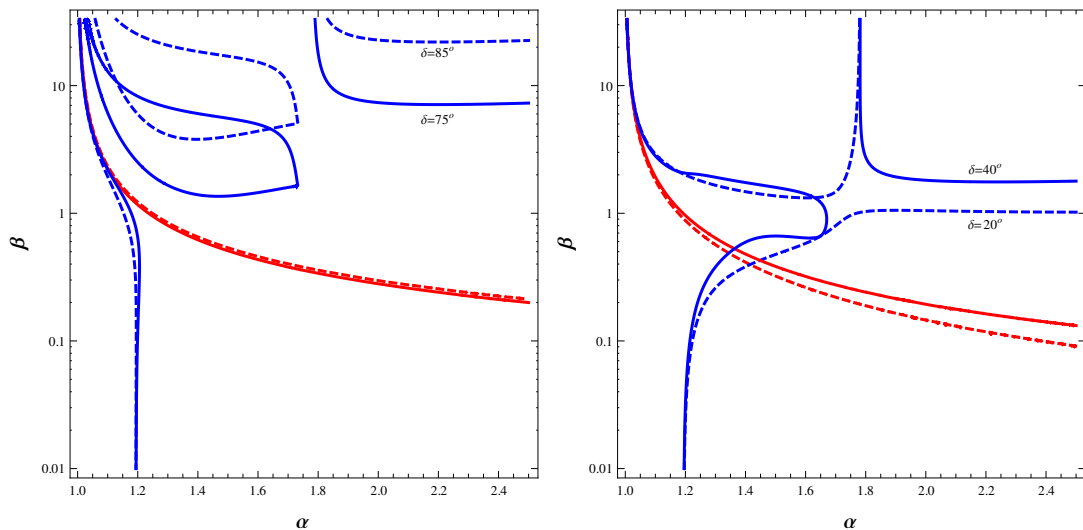


Figure 8: Contour plots r and $\sin^2 \theta_{13}$ when $\alpha > 1$. In the left panel dashed (continuous) line represents $\delta = 85^\circ$ (75°). Where as, in the right panel, continuous (dashed) lines represents contour plots for $\delta = 30^\circ$ (60°).

of $\sin^2 \theta_{13}$ and r . Once we restrict β to be below one, we find the solutions to exist for $\delta = 0^\circ - 63^\circ$, ($117^\circ - 180^\circ$, $180^\circ - 243^\circ$, $297^\circ - 360^\circ$) shown in Table 4. For δ 's beyond 63° (when considered within $\pi/2$), the solutions exhibit $\beta \gg 1$ implying a fine tuned situation similar to case A. Note that α therefore falls in a narrow range $\simeq 1.2 - 1.4$ in order to satisfy both $\sin^2 \theta_{13} = 0.0234$ and $r = 0.03$ considering all δ values. In Fig.(9), left panel, we find the intersection is at $(1.36, 0.53)$ for $\delta = 40^\circ$ ($\equiv 140^\circ, 220^\circ, 320^\circ$). Considering this δ as a reference for discussion, we further include the 3σ range of $\sin^2 \theta_{13}$ in Fig.9, right panel. We

δ	α	β	$\sum m_i(\text{eV})$
$10^\circ(170^\circ, 190^\circ, 350^\circ)$	1.43	0.36	0.0791
$30^\circ(150^\circ, 210^\circ, 330^\circ)$	1.39	0.45	0.0798
$40^\circ(140^\circ, 220^\circ, 320^\circ)$	1.36	0.53	0.0799
$50^\circ(130^\circ, 230^\circ, 310^\circ)$	1.32	0.64	0.0794
$60^\circ(120^\circ, 240^\circ, 300^\circ)$	1.26	0.83	0.0776
$70^\circ(110^\circ, 250^\circ, 290^\circ)$	1.17	1.13	0.0739
$73^\circ(107^\circ, 253^\circ, 287^\circ)$	1.07	3.02	0.0696

Table 4: Solutions for $\alpha(> 1)$ and β for various δ .

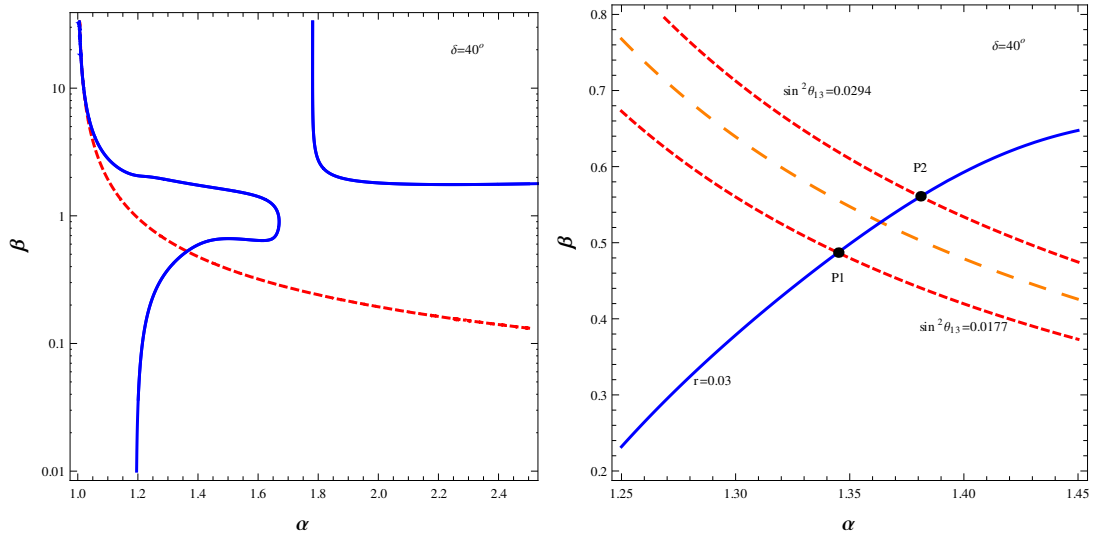


Figure 9: Contour plots of $r = 0.03$ and $\sin^2 \theta_{13} = 0.0234$ together in the $\alpha - \beta$ plane. In the right panel, the intersection region is elaborated where 3σ regions of $\sin^2 \theta_{13}$ are depicted.

find α to be varied between 1.35 and 1.39 while $\sin^2 \theta_{13}$ changes from the lower to the higher value, within 3σ limit. Within this range, we predict individual light neutrino masses and their sum. Here also we find normal hierarchy for them in Fig.10. For different δ -values, the Σm_i (corresponding to the best fit value of $\sin^2 \theta_{13}$) are provided in Table 4. For showing the prediction of our model in terms of other quantities like $|m_{ee}|$ and J_{CP} , the Fig.11, left and right panels are included. Considering all the δ values for which $\beta \leq 1$, we find $|J_{CP}|$ to be within $|J_{CP}| < 0.035$.

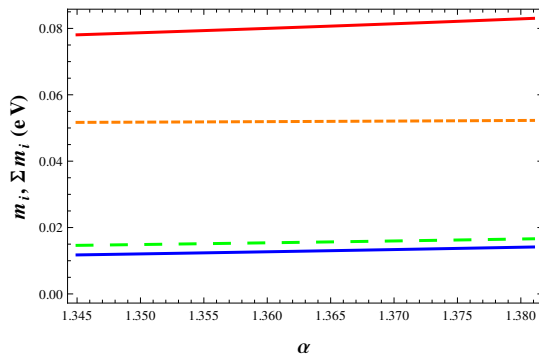


Figure 10: Neutrino masses vs α for $\delta = 40^\circ(140^\circ, 220^\circ, 320^\circ)$ when $\alpha > 1$

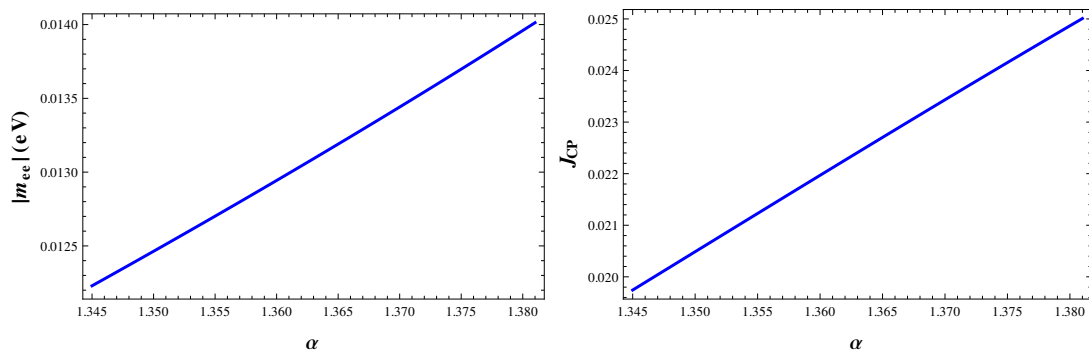


Figure 11: Effective neutrino mass parameter (left panel) and Jarlskog invariant (right panel) for $\delta = 40^\circ(140^\circ, 220^\circ, 320^\circ)$ when $\alpha > 1$.

5 Leptogenesis

In a general type-II seesaw framework, leptogenesis can be successfully implemented through the decay of RH neutrinos [66] or from the decay of the triplet(s) involved [67–71] or in a mixed scenario where both RH neutrino and the triplet(s) contribute [72–77]. In the present set-up, all the couplings involved in the pure type-I contribution are real and hence the neutrino Yukawa matrices and the RH neutrino mass matrices do not include any CP violating phase. Therefore CP asymmetry originated from the sole contribution of RH neutrinos is absent in our framework. As we have mentioned earlier, the source of CP violation is only present in the triplet contribution and that is through the vev of the S field. However as it is known [70, 79], a single $SU(2)_L$ triplet does not produce CP-asymmetry. Therefore there are two remaining possibilities to generate successful lepton asymmetry [74, 78] in the present context; (I) from the decay of the triplet where the one loop diagram involves the virtual RH neutrinos and (II) from the decay of the RH neutrinos where the one loop contribution involves the virtual triplet running in the loop. Provided the mass of the triplet is light compared to all the RH

neutrinos (*i.e.*, $M_\Delta < M_{Ri}$), we consider option (I). Once the triplet is heavier than the RH neutrinos, we explore option (II).

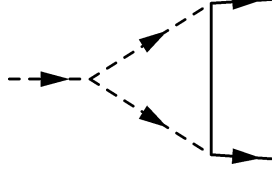


Figure 12: One-loop diagram which contributes to the generation of ϵ_Δ .

First we consider option (I), *i.e.*, when $M_\Delta < M_{Ri}$. At tree level the scalar triplet can decay either into leptons or into two Higgs doublets, followed from the Lagrangian in Eq.(3.8) and (3.11). For $\Delta \rightarrow LL$, the one loop diagram involves the virtual RH neutrinos running in the loop as shown in Fig. 12. Interference of the tree level and the one loop results in the asymmetry parameter [67, 74, 80]

$$\epsilon_\Delta = 2 \frac{\Gamma(\Delta^* \rightarrow L + L) - \Gamma(\Delta \rightarrow \bar{L} + \bar{L})}{\Gamma(\Delta^* \rightarrow L + L) + \Gamma(\Delta \rightarrow \bar{L} + \bar{L})}, \quad (5.1)$$

$$= \frac{1}{8\pi} \sum_k M_{Rk} \frac{\sum_{il} \text{Im}[(\hat{Y}_D^*)_{ki}(\hat{Y}_D)_{kl}(Y_\Delta)_{il}\eta^*]}{\sum_{ij} |(Y_\Delta)_{ij}|^2 M_\Delta^2 + |\eta|^2} \log(1 + M_\Delta^2/M_{Rk}^2). \quad (5.2)$$

Here i, j denote the flavor indices, $\hat{Y}_D = U_R^T Y_D$ in the basis where RH neutrino mass matrix is diagonal. Y_Δ, Y_D and expression of η can be obtained from Eqs.(3.5),(3.9) and (3.12). Masses of RH neutrinos can be expressed as

$$M_{R1} = \frac{v^2 y^2}{k} (1 + \alpha), \quad (5.3)$$

$$M_{R2} = \frac{v^2 y^2}{k}, \quad (5.4)$$

$$M_{R3} = \left| \frac{v^2 y^2}{k} (1 - \alpha) \right|. \quad (5.5)$$

Therefore, the asymmetry parameter in our model is estimated to be [74]

$$\epsilon_\Delta = -\frac{M_\Delta^2}{8\pi v^2} \frac{\alpha^2}{(1 - \alpha^2)} \frac{k\mu\tilde{\omega}^3 v_S (x_1 - x'_1) \sin \alpha_S}{\left[3\tilde{\omega}^2 \frac{v_S^2}{\Lambda^2} (x_1^2 + x'_1{}^2 + 2x_1 x'_1 \cos 2\alpha_S) M_\Delta^2 + (\mu\tilde{\omega}^2 \Lambda)^2 \right]}. \quad (5.6)$$

Here we denote $\tilde{\omega} = v_f/\Lambda$, where v_f is considered to be the common vev of all flavons except S -field's vev $\langle S \rangle = v_S e^{i\alpha_S}$. The associated phase α_S is the only source of CP-violation here. The total decay width of the triplet Δ (for $\Delta \rightarrow$ two leptons and $\Delta \rightarrow$ two scalar doublets)

is given by

$$\Gamma_T = \Gamma_{\Delta^* \rightarrow LL} + \Gamma_{\Delta^* \rightarrow HH} \quad (5.7)$$

$$= \frac{M_\Delta}{8\pi} \left[\sum_{ij} |(Y_\Delta)_{ij}|^2 + \frac{|\eta|^2}{M_\Delta^2} \right]. \quad (5.8)$$

Note that there are few parameters in Eq.(5.6), *e.g.* α, k which already contributed in determining the mass and mixing for light neutrinos. Also ϕ_d is related with α_S by Eq.(4.9). In the previous section, we have found solutions for (α, β) that satisfy the best fit values of $\sin^2 \theta_{13}$ and r for a specific choice of δ (the reference values $\delta = 80^\circ$ for $\alpha < 1$ and $\delta = 40^\circ$ for $\alpha > 1$). Then we can find the values of k and $|d|$ corresponding to that specific δ value. These set of $\alpha, |d|, k$ produce correct order of neutrino mass and mixing as we have already seen. Here to discuss the CP-asymmetry parameter ϵ_Δ , we therefore choose $\delta = 80^\circ (100^\circ, 260^\circ, 280^\circ)$ for $\alpha < 1$ and $\delta = 40^\circ (140^\circ, 220^\circ, 320^\circ)$ for $\alpha > 1$.

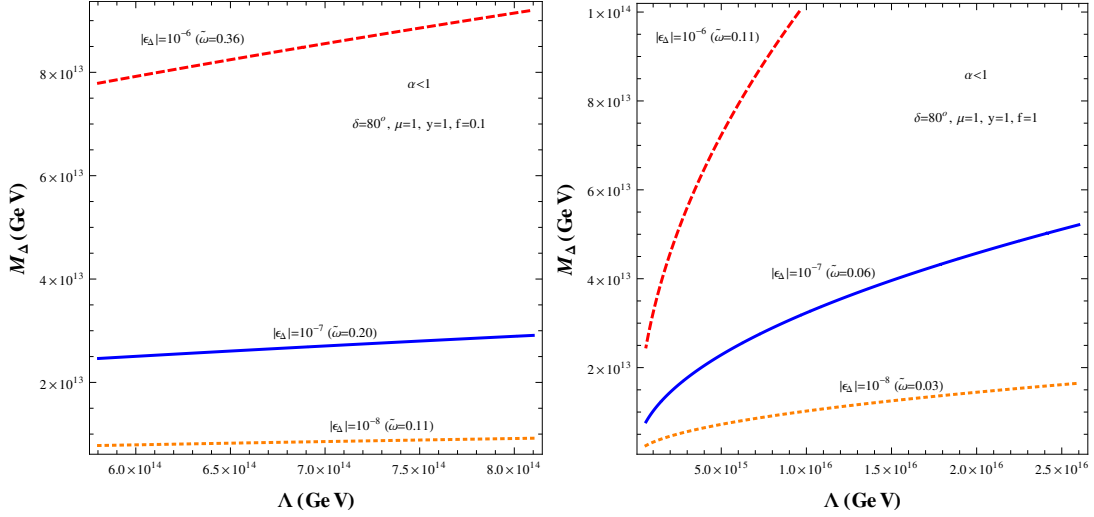


Figure 13: Contours of different values of ϵ_Δ in the $M_\Delta - \Lambda$ plane for $\alpha < 1$.

We further define $v_S/\Lambda = f\tilde{\omega}$ where f serves as a relative measure of the vevs. With this, the expression of ϵ_Δ takes the form

$$\epsilon_\Delta = -\frac{\alpha^2}{8\pi v^2(1-\alpha^2)} \frac{kf(x_1 - x'_1) \sin \alpha_S (\mu\Lambda/M_\Delta^2)}{[(3f^2/M_\Delta^2)(x_1^2 + x_1'^2 + 2x_1x_1' \cos 2\alpha_S) + (\mu\Lambda/M_\Delta^2)^2]}, \quad (5.9)$$

which is $\tilde{\omega}$ independent. The expression for $|d|$ as obtained from Eq. 3.14 can be written as

$$|d| = 2fv^2\tilde{\omega}^4 \frac{\mu\Lambda}{M_\Delta^2} (x_1 + x'_1) \cos \alpha_S \sec \phi_d. \quad (5.10)$$

Using Eq.(5.9), we obtain the contour plot for $\epsilon_\Delta = 10^{-6}, 10^{-7}, 10^{-8}$ with $\mu = 1, f = 0.1, x_1 = 0.5$ and $x'_1 = 1$ which are shown in Fig. 13, left panel. The electroweak vev is also

inserted in the expression. In obtaining the plots we varied Λ above the masses of RH neutrinos (see Eq.(5.5)). The variation of M_Δ is also restricted from above by the condition that we work in regime (I) where $M_\Delta < M_{Ri=1,2,3}$. Fig.13 is produced for a specific choice of $\delta = 80^\circ(100^\circ, 260^\circ, 280^\circ)$ which corresponds to the solution ($\alpha = 0.16, \beta = 0.11$). The values of $|d|$ and k corresponding to this set of (α, β) are found to be 0.0068 eV and 0.06 eV respectively. We have chosen $y = 1$ for the left panel of Fig.13. In order to keep $M_\Delta < M_{Ri} < \Lambda$, we find $M_\Delta \simeq 10^{13-14}$ GeV which produce the required amount of CP-asymmetry which in turn can generate enough lepton asymmetry.

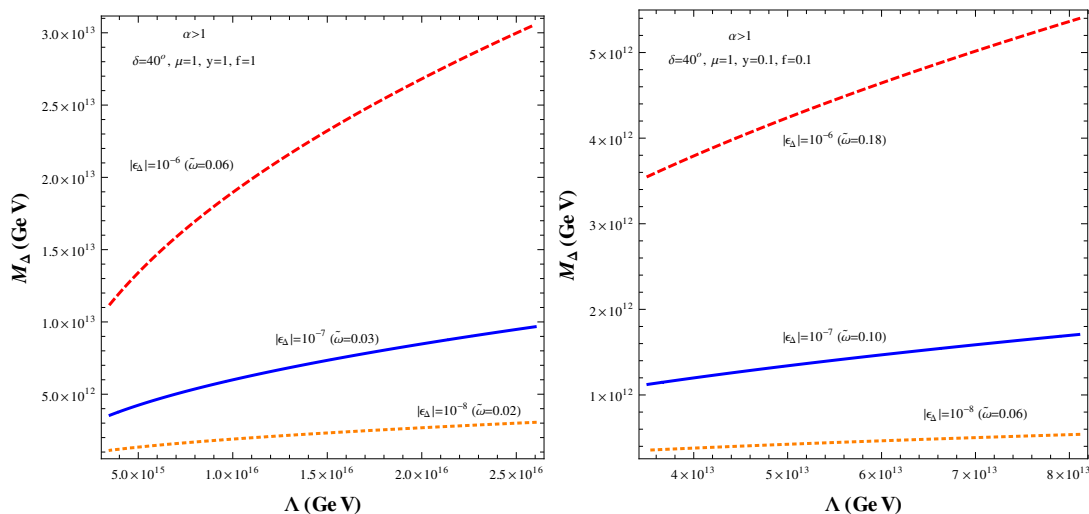


Figure 14: Contours of different values of ϵ_Δ in the $M_\Delta - \Lambda$ plane for $\alpha > 1$.

Note that value of $\tilde{\omega}$ can be concluded from the expression of $|d|$ in Eq.(5.10), for a choice of Λ/M_Δ^2 which produces a ϵ_Δ contour. This is because corresponding to a specific choice of δ value, $|d|$ is uniquely determined for the solution point (α, β). Hence with fixed values of x_1, x'_1, f, μ (with the same values to have the ϵ_Δ contour), $\tilde{\omega}$ can be evaluated from $|d|$ for a chosen Λ/M_Δ^2 . It turns out that $\tilde{\omega}$ has a unique value for a specific ϵ_Δ for both the panels of Fig.13. For example, with $\epsilon_\Delta = 10^{-7}$, we need $\tilde{\omega} = 0.2$, while to have $\epsilon_\Delta = 10^{-6}$, $\tilde{\omega}$ required to be 0.36. These $\tilde{\omega}$ values are provided in first bracket in each figure beside the ϵ_Δ value. The reason is the following. For the specified range of Λ (*i.e.* $M_\Delta < M_{Ri} < \Lambda$), it follows that the first bracketed term in the denominator of Eq.(5.9) is almost negligible compared to the second term (with the choice of x_1, x'_1, f, μ as mentioned before) and hence effectively

$$\epsilon_\Delta \simeq -\frac{\alpha^2}{8\pi v^2(1-\alpha^2)} k f (x_1 - x'_1) \sin \alpha_S \frac{M_\Delta^2}{\mu \Lambda}. \quad (5.11)$$

Therefore for a typical choice of ϵ_Δ , Λ/M_Δ^2 is almost fixed and then $|d|$ expression in Eq.(5.11) tells that $\tilde{\omega}$ also is almost fixed. In the right panel of Fig.13, we take $y = 1, f = 1$ and draw

the contours for ϵ_Δ while x_1, x'_1, μ are fixed at their previous values considered for generating plots in the left panel. In this case, M_Δ turns out to be 10^{13-14} GeV.

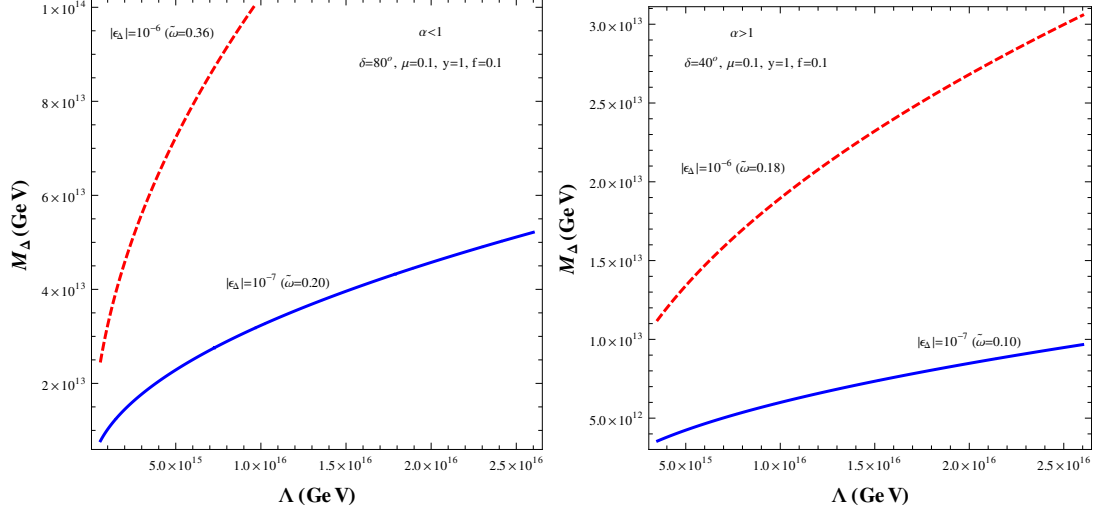


Figure 15: Contours of different values of ϵ_Δ in the $M_\Delta - \Lambda$ plane for $\alpha < 1$ (left panel) and $\alpha > 1$ (right panel) with small $\mu (= 0.1)$.

Similarly contours for ϵ_Δ are drawn in Fig.14 for $\alpha > 1$ case. Correspondingly we have used solutions of $(\alpha = 1.36, \beta = 0.53)$ and the value of $k = 0.02$ eV and $|d| = 0.01$ eV are taken for $\delta = 40^\circ$ (also for $140^\circ, 220^\circ, 320^\circ$). We obtain somewhat lighter M_Δ as correspond to the case with $\alpha < 1$. In Fig.15 similar contour plots for ϵ_Δ are exercised with μ at some lower values, fixed at $\mu = 0.1$ along with $f = 0.1$ for both $\alpha < 1$ and $\alpha > 1$.

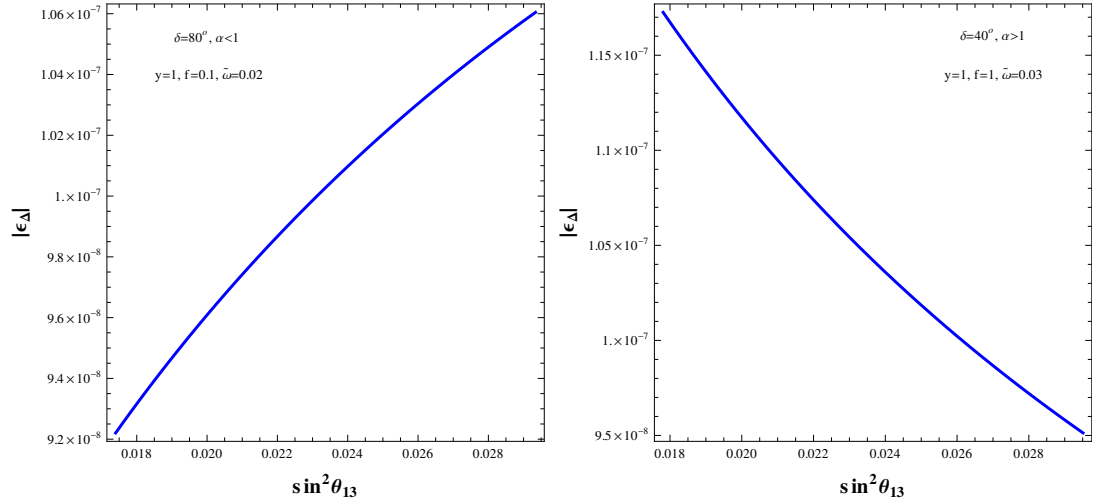


Figure 16: ϵ_Δ vs $\sin^2 \theta_{13}$ for $\alpha < 1$ (left panel) and $\alpha > 1$ (right panel).

So overall we have found that enough ϵ_Δ can be created so as to achieve the required

lepton asymmetry through $\frac{n_L}{n_\gamma} = \epsilon_\Delta \frac{n_\Delta}{n_\gamma} D$ with $n_\Delta = n_{\Delta_0} + n_{\Delta_+} + n_{\Delta_{++}}$ is the total number density of the triplet and D is the efficiency factor. After converting it into baryon asymmetry by the sphaleron process, n_B/n_γ is given by $\frac{n_B}{n_\gamma} \simeq -0.03\epsilon_\Delta D$. D depends on the satisfaction of the out-of-equilibrium condition ($\Gamma_\Delta \leq H|_{T=M_\Delta}$). Being $SU(2)_L$ triplet, it also contains the gauge interactions. Hence the scattering like $\Delta\Delta \rightarrow \text{SM particles}$ can be crucial [81, 82]. In [69, 70, 74, 83, 84], it has been argued that even if the triplet mass (M_Δ) is much below 10^{14} GeV, the triplet leptogenesis mechanism considered here is not affected much by the gauge mediated scatterings. However the exact estimate of D requires to solve the Boltzmann equations in detail which is beyond the scope of the present work. However analysis toward evaluating D in this sort of framework (where a single triplet is present and RH neutrinos are in the loop for generating ϵ_Δ) exits in [70]. Following [70], we note that with the effective type-II mass $\tilde{m}_\Delta \left(\equiv \sqrt{\text{Tr}(m_\nu^{II\dagger} m_\nu^{II})} \right) \sim (0.01 - 0.02) \text{ eV}$, the efficiency D is of the order of 10^{-3} . In estimating⁷ \tilde{m}_Δ , we have considered all the parameters in a range (mentioned within Fig. 13-14) so as to produce ϵ_Δ of order 10^{-6} as shown in Fig.13-14.

Now, using the approximated expression as given by Eq.(5.11) we can obtain variation of ϵ_Δ against $\sin^2 \theta_{13}$ as given in Fig. 16. In doing so we have substituted $\mu\Lambda/M_\Delta^2$ from Eq.(5.10) in Eq.(5.11). Then as discussed in the previous section, using solutions for α, β for 3σ range of $\sin^2 \theta_{13}$ for fixed δ we have obtained Fig.16 for both $\alpha < 1$ and $\alpha > 1$. Here the left panel is for $\delta = 80^\circ(100^\circ, 260^\circ, 280^\circ)$ and right panel in for $\delta = 40^\circ(140^\circ, 220^\circ, 320^\circ)$.

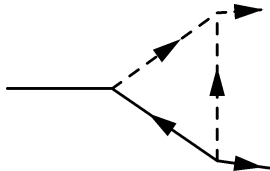


Figure 17: One-loop diagram for decay of RH neutrinos

We now discuss the option II, when RH neutrinos are lighter than M_Δ . The contribution toward the CP-asymmetry parameter generated from the decay of the lightest neutrino is

⁷It is possible to recast Eq.(5.2) as $\epsilon_\Delta = -\frac{1}{8\pi} \frac{M_\Delta}{v^2} \sqrt{B_L B_H} \frac{\text{Tr}(m_\nu^{I\dagger} m_\nu^{II})}{\tilde{m}_\Delta}$ with the consideration $M_\Delta < M_{Rk}$. Here B_L and B_H are corresponding branching ratio's of decay of the triplet into two leptons and two scalar doublets.

given by

$$\epsilon_{N_1} = -\frac{1}{8\pi v^2} M_{R_1} \frac{\sum_{il} \text{Im}[(\hat{Y}_D)_{1i}(\hat{Y}_D)_{1l}(m_\nu^{II*})_{il}]}{\sum_i |(\hat{Y}_D)_{1i}|^2}, \quad (5.12)$$

$$= -\frac{M_{R_1}}{2} \frac{1}{8\pi v^2} |d| \sin \phi_d, \quad (5.13)$$

$$\epsilon_{N_2} = M_{R_2} \frac{1}{8\pi v^2} |d| \sin \phi_d \quad \text{and} \quad \epsilon_{N_3} = \pm \frac{M_{R_3}}{2} \frac{1}{8\pi v^2} |d| \sin \phi_d. \quad (5.14)$$

where we have used m_ν^{II} from Eq.(3.13). In the above, ‘+’ and ‘-’ sign stands for $\alpha > 1$ and $\alpha < 1$ cases respectively in computation of ϵ_{N_3} . Note that in the present scenario the RH neutrino masses are not entirely hierarchical, rather they are closely placed. therefore the total baryon asymmetry from the decay of the three RH neutrinos is to be estimated as $|\frac{n_B}{s}| = 1.48 \times 10^{-3} \sum_i \epsilon_{N_i} D_{N_i}$, where D_{N_i} is the respective efficiency factor. It turns out that with the same D_{N_i} for $i = 1, 2, 3$, $\sum_i \epsilon_{N_i} = 0$ as a result (using M_{R_i} from Eq.(5.5)) of the specific flavor structure considered. Therefore it is expected that the lepton asymmetry would be suppressed in this case. Also in this case $M_{R_i} < M_\Delta$, which can be obtained by considering smaller value of the Yukawa coupling y (as to generate the required $|d|$, specific values of α, β, k are already chosen). This could reduce the individual ϵ_{N_i} . We conclude this contribution (ϵ_N) as a subdominant to ϵ_Δ .

6 Conclusion

We have considered a flavor symmetric framework for generating light neutrino masses and mixing through type-II seesaw mechanism. In realizing it, we have introduced three SM singlet RH neutrinos, one $SU(2)_L$ triplet and few flavon fields. The RH neutrinos contribute to the type-I term, which guided by the $A_4 \times Z_4 \times Z_3$ symmetry of the model produces a TBM mixing pattern. Then we have shown that the typical flavor structure resulted from the model can generate nonzero θ_{13} . In this framework, all the couplings are considered to be real. The CP symmetry is violated spontaneously by the complex vev of a single SM singlet field, while other flavons have real vevs. Interestingly this particular field is involved only in the pure type-II term. Hence the triplet contribution not only generates the θ_{13} , it is also responsible for providing Dirac CP violating phase δ . Therefore the model has the potential to predict δ in terms of the parameters involved in neutrino masses and mixing. We have therefore studied the parameter space of the set-up considering that the triplet contribution is subdominant or at most comparable to the type-I term. The model indicates the values of δ to be in the range $72^\circ - 82^\circ, 98^\circ - 108^\circ, 252^\circ - 262^\circ, 278^\circ - 288^\circ$ for $\alpha < 1$ and $\delta = 0^\circ - 63^\circ, 117^\circ - 180^\circ, 180^\circ - 243^\circ, 297^\circ - 360^\circ$ for $\alpha > 1$. However $\delta = 0$ (and hence $\pi, 2\pi$) is disfavored in our scenario as in that case no CP violation would be present. Also $\delta = \pi/2, 3\pi/2$ are excluded

here. These ranges can be tested in future neutrino experiments. We provide an estimate for the J_{CP} . The sum of the neutrino masses are also evaluated. It turns out that the scenario works with normal hierarchical masses of light neutrinos. We have also studied leptogenesis in this model. As the type-I contribution to the light neutrino mass does not involve any CP violating phase, RH neutrinos decay can not contribute to the lepton asymmetry in the conventional way. We have found the triplet decay with the virtual RH neutrino in the loop can produce enough lepton asymmetry.

References

- [1] P. Minkowski, Phys. Lett. B **67**, 421 (1977).
- [2] M. Gell-Mann, P. Ramond and R. Slansky, Conf. Proc. C **790927**, 315 (1979) [arXiv:1306.4669 [hep-th]].
- [3] R. N. Mohapatra and G. Senjanovic, Phys. Rev. Lett. **44**, 912 (1980).
- [4] T. Yanagida, Prog. Theor. Phys. **64**, 1103 (1980).
- [5] P. F. Harrison, D. H. Perkins and W. G. Scott, Phys. Lett. B **458**, 79 (1999) [hep-ph/9904297].
- [6] E. Ma, Phys. Rev. D **70**, 031901 (2004) [hep-ph/0404199].
- [7] G. Altarelli and F. Feruglio, Nucl. Phys. B **720**, 64 (2005) [hep-ph/0504165].
- [8] G. Altarelli and F. Feruglio, Nucl. Phys. B **741**, 215 (2006) [hep-ph/0512103].
- [9] Y. Abe *et al.* [DOUBLE-CHOOZ Collaboration], Phys. Rev. Lett. **108**, 131801 (2012) [arXiv:1112.6353 [hep-ex]].
- [10] F. P. An *et al.* [DAYA-BAY Collaboration], Phys. Rev. Lett. **108**, 171803 (2012) [arXiv:1203.1669 [hep-ex]]; F. P. An *et al.* [Daya Bay Collaboration], arXiv:1406.6468 [hep-ex].
- [11] J. K. Ahn *et al.* [RENO Collaboration], Phys. Rev. Lett. **108**, 191802 (2012) [arXiv:1204.0626 [hep-ex]].
- [12] K. Abe *et al.* [T2K Collaboration], Phys. Rev. Lett. **112**, 061802 (2014) [arXiv:1311.4750 [hep-ex]].
- [13] B. Karmakar and A. Sil, Phys. Rev. D **91**, 013004 (2015) [arXiv:1407.5826 [hep-ph]].

- [14] A. S. Joshipura and E. A. Paschos, hep-ph/9906498.
- [15] A. S. Joshipura, E. A. Paschos and W. Rodejohann, Nucl. Phys. B **611**, 227 (2001) [hep-ph/0104228].
- [16] B. Bajc, G. Senjanovic and F. Vissani, Phys. Rev. Lett. **90**, 051802 (2003) [hep-ph/0210207].
- [17] S. Antusch and S. F. King, Nucl. Phys. B **705**, 239 (2005) [hep-ph/0402121].
- [18] S. Antusch and S. F. King, Phys. Lett. B **597**, 199 (2004) [hep-ph/0405093].
- [19] N. Sahu and S. U. Sankar, Phys. Rev. D **71**, 013006 (2005) [hep-ph/0406065].
- [20] W. Rodejohann and Z. z. Xing, Phys. Lett. B **601**, 176 (2004) [hep-ph/0408195].
- [21] S. L. Chen, M. Frigerio and E. Ma, Nucl. Phys. B **724**, 423 (2005) [hep-ph/0504181].
- [22] S. Bertolini and M. Malinsky, Phys. Rev. D **72**, 055021 (2005) [hep-ph/0504241].
- [23] E. K. Akhmedov and M. Frigerio, JHEP **0701**, 043 (2007) [hep-ph/0609046].
- [24] W. Rodejohann, Phys. Rev. D **70**, 073010 (2004) [hep-ph/0403236].
- [25] P. H. Gu, H. Zhang and S. Zhou, Phys. Rev. D **74**, 076002 (2006) [hep-ph/0606302].
- [26] A. Abada, P. Hosteins, F. X. Josse-Michaux and S. Lavignac, Nucl. Phys. B **809**, 183 (2009) [arXiv:0808.2058 [hep-ph]].
- [27] D. Borah and M. K. Das, Phys. Rev. D **90**, no. 1, 015006 (2014) [arXiv:1303.1758 [hep-ph]].
- [28] D. Borah, Int. J. Mod. Phys. A **29**, 1450108 (2014) [arXiv:1403.7636 [hep-ph]].
- [29] M. Borah, D. Borah, M. K. Das and S. Patra, Phys. Rev. D **90**, no. 9, 095020 (2014) [arXiv:1408.3191 [hep-ph]].
- [30] R. Kalita, D. Borah and M. K. Das, Nucl. Phys. B **894**, 307 (2015) [arXiv:1412.8333 [hep-ph]].
- [31] S. Pramanick and A. Raychaudhuri, arXiv:1508.02330 [hep-ph].
- [32] M. Magg and C. Wetterich, Phys. Lett. B **94**, 61 (1980).
- [33] G. Lazarides, Q. Shafi and C. Wetterich, Nucl. Phys. B **181**, 287 (1981).

- [34] R. N. Mohapatra and G. Senjanovic, Phys. Rev. D **23**, 165 (1981).
- [35] J. Schechter and J. W. F. Valle, Phys. Rev. D **22**, 2227 (1980).
- [36] F. Capozzi, G. L. Fogli, E. Lisi, A. Marrone, D. Montanino and A. Palazzo, Phys. Rev. D **89**, no. 9, 093018 (2014) [arXiv:1312.2878 [hep-ph]].
- [37] M. C. Gonzalez-Garcia, M. Maltoni and T. Schwetz, JHEP **1411**, 052 (2014) [arXiv:1409.5439 [hep-ph]].
- [38] D. V. Forero, M. Tortola and J. W. F. Valle, Phys. Rev. D **90**, no. 9, 093006 (2014) [arXiv:1405.7540 [hep-ph]].
- [39] T. D. Lee, Phys. Rev. D **8**, 1226 (1973).
- [40] A. E. Nelson, Phys. Lett. B **136**, 387 (1984).
- [41] S. M. Barr, Phys. Rev. Lett. **53**, 329 (1984).
- [42] J. A. Harvey, P. Ramond and D. B. Reiss, Phys. Lett. B **92**, 309 (1980).
- [43] J. A. Harvey, D. B. Reiss and P. Ramond, Nucl. Phys. B **199**, 223 (1982).
- [44] G. C. Branco, Phys. Rev. D **22**, 2901 (1980).
- [45] L. Bento and G. C. Branco, Phys. Lett. B **245**, 599 (1990).
- [46] L. Bento, G. C. Branco and P. A. Parada, Phys. Lett. B **267**, 95 (1991).
- [47] G. C. Branco, P. A. Parada and M. N. Rebelo, hep-ph/0307119.
- [48] G. C. Branco, R. Gonzalez Felipe, F. R. Joaquim and H. Serodio, Phys. Rev. D **86**, 076008 (2012) [arXiv:1203.2646 [hep-ph]].
- [49] G. C. Branco, T. Morozumi, B. M. Nobre and M. N. Rebelo, Nucl. Phys. B **617**, 475 (2001) [hep-ph/0107164].
- [50] T. Araki and H. Ishida, PTEP **2014**, no. 1, 013B01 (2014) [arXiv:1211.4452 [hep-ph]].
- [51] Y. H. Ahn, S. K. Kang and C. S. Kim, Phys. Rev. D **87**, no. 11, 113012 (2013) [arXiv:1304.0921 [hep-ph]].
- [52] J. E. Kim and S. Nam, arXiv:1506.08491 [hep-ph].
- [53] Y. Achiman, Phys. Lett. B **599**, 75 (2004) [hep-ph/0403309].

- [54] Y. Achiman, Phys. Lett. B **653**, 325 (2007) [hep-ph/0703215].
- [55] M. Frank, Phys. Rev. D **70**, 036004 (2004).
- [56] M. C. Chen and K. T. Mahanthappa, Phys. Rev. D **71**, 035001 (2005) [hep-ph/0411158].
- [57] N. Sahu and S. U. Sankar, Nucl. Phys. B **724**, 329 (2005) [hep-ph/0501069].
- [58] W. Chao, S. Luo and Z. z. Xing, Phys. Lett. B **659**, 281 (2008) [arXiv:0704.3838 [hep-ph]].
- [59] K. A. Olive *et al.* [Particle Data Group Collaboration], Chin. Phys. C **38**, 090001 (2014).
- [60] S. Fukuda *et al.* [Super-Kamiokande Collaboration], Phys. Lett. B **539**, 179 (2002) [hep-ex/0205075]; Y. Ashie *et al.* [Super-Kamiokande Collaboration], Phys. Rev. D **71**, 112005 (2005) [hep-ex/0501064]. P. Adamson *et al.* [MINOS Collaboration], Phys. Rev. Lett. **106**, 181801 (2011) [arXiv:1103.0340 [hep-ex]]. T. Araki *et al.* [KamLAND Collaboration], Phys. Rev. Lett. **94**, 081801 (2005) [hep-ex/0406035].
- [61] P. A. R. Ade *et al.* [Planck Collaboration], arXiv:1303.5076 [astro-ph.CO].
- [62] K. Asakura *et al.* [KamLAND-Zen Collaboration], AIP Conf. Proc. **1666**, 170003 (2015) [arXiv:1409.0077 [physics.ins-det]].
- [63] J. B. Albert *et al.* [EXO-200 Collaboration], Nature **510**, 229 (2014) [arXiv:1402.6956 [nucl-ex]].
- [64] S. F. King and C. Luhn, JHEP **1109**, 042 (2011) [arXiv:1107.5332 [hep-ph]].
- [65] G. Altarelli, F. Feruglio and L. Merlo, Fortsch. Phys. **61**, 507 (2013) [arXiv:1205.5133 [hep-ph]].
- [66] For a review, see S. Davidson, E. Nardi and Y. Nir, Phys. Rept. **466**, 105 (2008) [arXiv:0802.2962 [hep-ph]] and references there in.
- [67] P. J. O'Donnell and U. Sarkar, Phys. Rev. D **49**, 2118 (1994) [hep-ph/9307279].
- [68] E. Ma and U. Sarkar, Phys. Rev. Lett. **80**, 5716 (1998) [hep-ph/9802445];
- [69] T. Hambye, E. Ma and U. Sarkar, Nucl. Phys. B **602**, 23 (2001) [hep-ph/0011192];
- [70] T. Hambye, M. Raidal and A. Strumia, Phys. Lett. B **632**, 667 (2006) [hep-ph/0510008].
- [71] G. C. Branco, R. G. Felipe and F. R. Joaquim, Rev. Mod. Phys. **84**, 515 (2012) [arXiv:1111.5332 [hep-ph]].

- [72] D. Aristizabal Sierra, F. Bazzocchi, I. de Medeiros Varzielas, L. Merlo and S. Morisi, Nucl. Phys. B **827**, 34 (2010) [arXiv:0908.0907 [hep-ph]].
- [73] D. Aristizabal Sierra and I. de Medeiros Varzielas, Fortsch. Phys. **61**, 645 (2013) [arXiv:1205.6134 [hep-ph]].
- [74] T. Hambye and G. Senjanovic, Phys. Lett. B **582**, 73 (2004) [hep-ph/0307237].
- [75] S. Antusch, Phys. Rev. D **76**, 023512 (2007) [arXiv:0704.1591 [hep-ph]].
- [76] E. K. Akhmedov and W. Rodejohann, JHEP **0806**, 106 (2008) [arXiv:0803.2417 [hep-ph]].
- [77] D. Aristizabal Sierra, F. Bazzocchi and I. de Medeiros Varzielas, Nucl. Phys. B **858**, 196 (2012) [arXiv:1112.1843 [hep-ph]].
- [78] D. Aristizabal Sierra, M. Dhen and T. Hambye, JCAP **1408**, 003 (2014) [arXiv:1401.4347 [hep-ph]].
- [79] T. Hambye, New J. Phys. **14**, 125014 (2012) [arXiv:1212.2888 [hep-ph]].
- [80] G. Lazarides and Q. Shafi, Phys. Rev. D **58**, 071702 (1998) [hep-ph/9803397].
- [81] J. N. Fry, K. A. Olive and M. S. Turner, Phys. Rev. D **22**, 2977 (1980).
- [82] E. Ma, S. Sarkar and U. Sarkar, Phys. Lett. B **458**, 73 (1999) [hep-ph/9812276].
- [83] T. Hambye, hep-ph/0412053.
- [84] T. Hambye, Y. Lin, A. Notari, M. Papucci and A. Strumia, Nucl. Phys. B **695**, 169 (2004) [hep-ph/0312203].